EUROPEAN JOURNAL OF BIOMEDICAL AND PHARMACEUTICAL SCIENCES
http://www.ejbps.com

ISSN 2349-8870
Volume: 3
Issue: 1
259-264
Year: 2016

A STUDY ON BACTERIAL ISOLATES FROM DACRYOCYSTITIS PATIENTS IN A TERTIARY CARE TEACHING HOSPITAL KOLKATA, WEST BENGAL

Nilay Chatterjee[*1], Pinaki Biswas[1], Dr. Kumkum Bhattacharyya[2], Dr. Saurabh Laskar[3], Dr. Anita Nandi (Mitra)[4]

[1]Department of Microbiology, The University of Burdwan, Burdwan – 713104.
[2]Department of Microbiology, Murshidabad Medical College, Murshidabad – 742101.
[3]Department of Microbiology, R. G. Kar Medical College & Hospital, Kolkata – 700004.
[4]Department of Microbiology, Kolkata Medical College & Hospital, Kolkata – 700073.

***Author for Correspondence: Nilay Chatterjee**
Department of Microbiology, The University of Burdwan, Burdwan – 713104.

Article Received on 01/11/2015 **Article Revised on 22/11/2015** **Article Accepted on 12/12/2015**

ABSTRACT

Background: Dacryocystitis is one of the most common diseases of eye occurring due to inflammation of the lacrimal sac. It can be of two types: congenital and acquired. Acquired dacryocystitis can be divided into two groups: acute and chronic. Congenital dacryocystitis seen in new born are due to obstruction of the nasolacrimal duct by epithelial debris which produces hindrance in the flow of lacrimal fluid which encourages microbial growth. On the other hand, acute dacryocystitis is more common in women of middle age. Poor hygiene, pond bathing might be the source of infection causing acute infection in nasolacrimal duct resulting in swelling, inflammation, epiphora, and accumulation of pus. **Study design:** Fifty nine clinically diagnosed patients of dacryocystitis of all age groups and of both sexes were used for the study. Specimens were collected with the help of ophthalmologist. All specimens were subjected to gram staining followed by culture. Antibiotic susceptibility testing was done by Kirby-Bauer disc diffusion method as per CLSI guidelines. **Result:** Females are more affected than male and highest number of dacryocystitis cases are found among people in the age group of 46 – 60 years. Out of 59 cases of dacryocystitis 9 bacterial isolates were found of which 4 isolates were gram positive and 5 isolates were gram negative organisms. Antibiotic susceptibility tests shows that gram positive isolates were sensitive to vancomycin, oxacillin, linezolid and clindamycin followed by trimethoprim/sulfamethoxazole and gentamicin. Gram negative organisms were mostly sensitive to cefepime followed by amikacin, ceftazidime and piperacilin. **Conclusion:** The present study revealed that chronic dacryocystitis is the predominant clinical entity found mostly in elderly women. The causative organisms though varied show a predominance of Pseudomonas in our study.

KEYWORDS: Dacryocystitis, Pseudomonas aeruginosa, MSSA.

INTRODUCTION

Dacryocystitis is one of the most common diseases of the eye. It is an important cause of ocular morbidity both in children and adult.[1] Dacryocystitis is an inflammation of the lacrimal sac. It may be congenital and acquired. Acquired dacryocystitis are of 2 categories: acute and chronic.[2] Congenital dacryocystitis develop due to obstruction of the nasolacrimal duct, the block usually being due to the presence of epithelial debris or a membranous occlusion of the lower third of nasolacrimal duct. Blockage of the duct leads to stasis of the lacrimal fluid which harbors many organisms leading to infection. The obstruction may be unilateral or bilateral and is seen after birth, with the mother complaining of epiphora and discharge from the eyes of the child. The treatment, if started early, is easy and effective resulting in over a 90% cure rate. If the child is seen within 6 months after birth, the mother is instructed to perform sac massage and frequent installation of antibiotic drops. If this treatment is not successful and the epiphora is persistent even after 4 weeks of proper treatment, probing of the nasolacrimal duct is performed under general anesthesia. It may sometimes be necessary to perform several probing in order to open the nasolacrimal duct. However, if probing also fail to open the block, dacryocystorhinostomy is performed when the child reaches the age of three years.[3] Acute dacryocystitis occurs more often in women and patient complains of tearing and pain followed by acute onset of swelling in the lacrimal sac fossa region with oedema spreading over the lower lid and cheek. *Streptococcus* species are the most commonly isolated organisms in acute dacryocystitis. It is treated by systemic antibiotics, systemic anti-inflammatory drugs and local hot

compresses.[4] Chronic dacryocystitis may present with a variety of symptoms, including unilateral tearing and intermittent milky discharge that accumulates in the inner canthus.[5] A non-tender mass in the medial canthus that is reducible by finger pressure is a common complaint. The most common organisms cultured in chronic dacryocystitis include *Staphylococcus aureus*, *Pneumococcus*, β-haemolytic *Streptococcus*, *Pseudomonas*, *Klebsiella* and other *Enterobacteriaceae*. Definitive treatment of chronic dacryocystitis is achieved with dacryocystorhinostomy.[6] If treatment is started early, progression to chronicity or the period of chronicity can be reduced and microbial resistance can be reduced by administering the antibiotics for which the organisms are susceptible.[7] During the past years there have been only a few studies conducted on the bacteriology of dacryocystitis and the information available is meager. Hence this study is being undertaken.

MATERIALS AND METHODS

This study is carried out in the department of microbiology, in a tertiary care teaching hospital in Kolkata, eastern India from May 2011 to July 2011. Clinically diagnosed cases of dacryocystitis attending ophthalmology out-patient department were taken for the study. Clinical history of all the patients like age, sex, occupation and socioeconomic status of patient, nature and duration of symptoms, was included. Patients who had received either topical or systemic antibiotics for the past one week from their visit to the hospital were excluded. After clinical diagnosis of dacryocystitis by ophthalmologist, specimens were collected with the help of ophthalmologist. The surrounding area is aseptically cleaned to avoid contamination from the surface microorganisms and samples were collected in two sterile cotton swabs from lacrimal sac. It is collected either by applying pressure over the lacrimal sac and allowing the purulent material to reflux through the lacrimal punctum or by irrigating the lacrimal drainage system with sterile saline called as Lacrimal Syringing and collecting the sample from the refluxing material ensuring that the lid margins or the conjunctiva were not touched. Another sample was collected from the conjunctival sac. In cases of acute lacrimal abscess on chronic dacryocystitis pus was drained and taken for culture.

All specimens were subjected to gram staining followed by culture. The specimens were inoculated into Nutrient agar, Blood agar and MacConkey agar and incubated at 37^{o}C for 18-24 hours. Each different type of colony on the media were identified by biochemical tests such as catalase, oxidase, indole production, methyl red, voges-proskauer, citrate utilization, urease hydrolysis, triple sugar iron (TSI) agar and carbohydrate fermentation (glucose, lactose, manitol, sucrose) tests. The specific tests like inulin fermentation, optochin sensitivity test and bile solubility test was used to identify *Streptococcus pneumoniae*. Slide and tube coagulase test was used to identify *Staphylococcus aureus*. Antimicrobial susceptibility testing was done by Kirby-Bauer disc diffusion method as per CLSI guidelines. Antibiotic discs obtained commercially (manufacturer- Hi-media laboratories, Mumbai) used were Amikacin (30mcg), Clindamycin (2mcg), Ciprofloxacin (RC, 5mcg), Cefepime (30mcg), Ceftazidime (30mcg), Erythromycin (15mcg), Gentamicin (10mcg), Imipenem (10mcg), Levofloxacin (5mcg), Linezolid (30mcg), Oxicillin (1mcg), Piperacillin (PC, 100mcg), Trimethoprim-sulfamethoxazole (30mcg), Vancomycin (5mcg).

RESULTS AND ANALYSIS

In the present study 59 clinically diagnosed patients of dacryocystitis of all age groups and of both sexes were studied over a period of 3 months (May 2011 to July 2011). Out of 59 cases under the study, it is observed that the females were affected more i.e., 44(74.58%) as compared to males 15(25.42%). The male to female ratio was 1: 2.93. In congenital dacryocystitis, females are more (10.17%) as compared to males (3.39%). In acquired dacryocystitis, females are more (64.40%) as compared to males (22.04%).

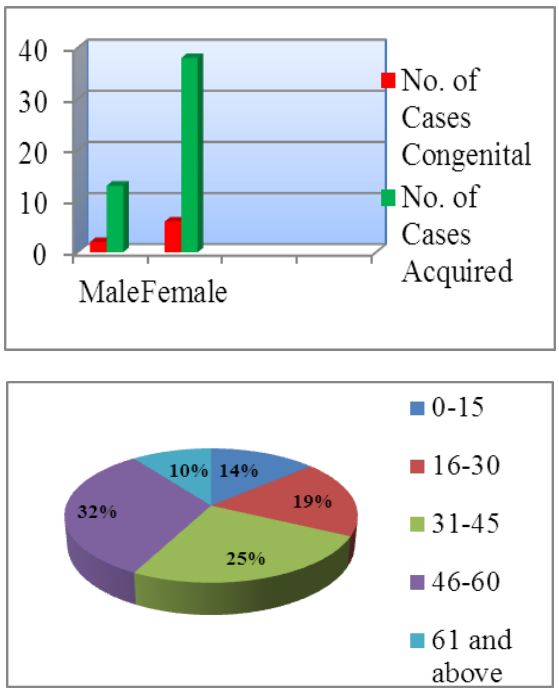

Fig No. 1: Graphic representation of distribution of dacryocystitis cases according to sex and age.

This series of study shows highest number of dacryocystitis cases among people in the age group of 46 – 60 years (32.20%). Next common age groups in sequence are 31 – 45 years (25.42%). The occurrences in 61 and above are 10.18%, 16 – 30 years 18.64% and 0 – 15 years is 13.56%. The youngest among the case studied was 5 years old and the oldest being 76 years. Among the total number of 59 cases the left eye affected was 29(49.15%) and that of right eye 20(33.89%) and bilateral 10(16.97%) cases. These statistics show that on the whole left eye is more affected than the right. As

regards the incidence of the left eye affected in female population was 26/44 cases, as against 13/44 cases having right eye affection. But when male to female ratio was compared, the proportion of females having left eye affected was 8.7 times that of males having left eye affected whereas the right eye affection is 1.9 times and bilateral is of 1 times affection.

Table 1: Distribution of dacryocystitis cases according to sex and eye affected.

Sl. No.	Eye affected	Unilateral cases		Bilateral cases
		Right	Left	
1	Males	7 (11.86%)	3 (5.08%)	5 (8.47%)
2	Females	13 (22.03%)	26 (44.06%)	5 (8.47%)
Total		20 (33.89%)	29 (49.15%)	10 (16.97%)

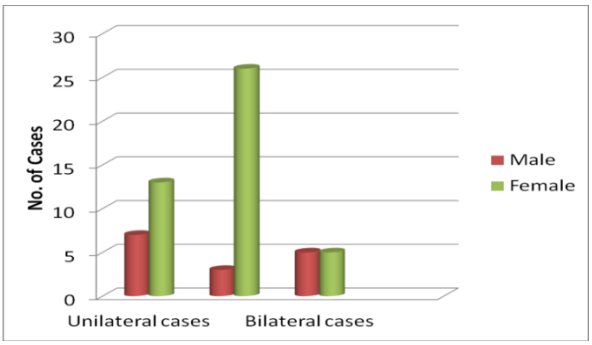

Fig No. 2: Distribution of dacryocystitis cases according to sex and eye affected.

Chronic dacryocystitis was most common clinical entity encountered in the present study comprising of 33(55.93%) cases while 18(30.51%) patients had acute dacryocystitis. Congenital dacryocystitis constitutes the third most common clinical presentation 8(13.56%) in this study.

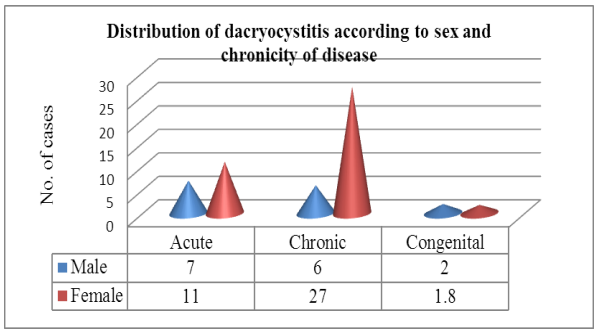

Fig No. 3: Distribution of dacryocystitis cases according to sex and chronicity of disease.

Out of 59 samples collected with a clinical diagnosis of dacryocystitis, there were 9 bacterial isolates altogether, 4 of which were of gram-positive bacteria, (45%) and 5 isolates were gram-negative bacteria (55%). The most frequent gram- positive isolate were Methicilin Sensitive *Staphylococcus aureus* (MSSA), which represented 3(5.08%) of total samples, followed by *Streptococcus pneumoniae* 1(1.69%). The most frequent gram-negative isolate were *Pseudomonas aeruginosa*, which represented 4(6.77%) of the total samples followed by *Acinetobacter baumannii* 1(1.69%).

Table2: Distribution of dacryocystitis cases according to spectrum of gram-positive organisms.

Sl. No.	Organisms	No. of Cases		Total No. (%)
		Congenital (8)	Acquired (51)	
1	*Staphylococcus aureus* (MSSA)	0	3	3 (5.08)
2	*Streptococcus pneumoniae*	0	1	1 (1.69)
Total		0	4	4 (6.78)

Table 3: Distribution of dacryocystitis cases according to spectrum of gram-negative organisms.

Sl. No.	Organisms	No. of Cases		Total No. (%)
		Congenital (8)	Acquired (51)	
1	*Pseudomonas aeruginosa*	1	3	4 (6.77)
2	*Acinetobacter baumannii*	0	1	1 (1.69)
Total		1	4	5 (8.47)

All the types of dacryocystitis i.e., 51 cases of acquired dacryocystitis and 8 cases of congenital dacryocystitis showed a preponderance of gram-negative organisms. Methicilin Sensitive *Staphylococcus aureus* (MSSA) was the predominant gram-positive organism in chronic dacryocystitis. *Pseudomonas aeruginosa* was the most common gram-negative isolate in both acute and congenital dacryocystitis. Out of 59 cases 9 patients have an active habit of pond bathing in which 3 have acute dacryocystitis and 6 have chronic dacryocystitis. In these cases, 2 acute cases are culture positive for *Pseudomonas aeruginosa* and 3 chronic cases are culture positive for *Staphylococcus aureus* (2) and *Acinetobacter baumannii*(1).

Table 4: Antibiotic susceptibility pattern of *Staphylococcus aureus* and *Pseudomonas aeruginosa.*

Isolates	Ciprofloxacin	Clindamycin	Erythromycin	Gentamicin	levofloxacin	Linezolid	Oxacillin	Trimethoprim/ Sulfamethoxazole	Vancomycin
S.aureus (3)	0 (0%)	3 (100%)	3 (100%)	1 (33.3%)	0 (0%)	3 (100%)	3 (100%)	2 (66.6%)	3 (100%)
	Amikacin	Ciprofloxacin	Cefepime	Ceftazidime	Gentamicin	levofloxacin	Piperacilin	Imipenem	Trimethoprim/ Sulfamethoxazole
P. Aeruginosa (4)	2 (50%)	1 (25%)	3 (75%)	2 (50%)	1 (25%)	1 (25%)	2 (50%)	1 (25%)	0 (0%)

The antibiotic susceptibility test shows that gram-positive isolates were most sensitive to vancomycin, oxacillin, linezolid, erythromycin and clindamycin (100%), followed by trimethoprim/sulfamethoxazole (66.6%) and gentamicin (33.3%). Ciprofloxacin and levofloxacin were resistant to all gram positive isolates. The gram-negative organisms were most sensitive to cefepime (75%), followed by amikacin, ceftazidime and piperacilin (50%). The least sensitive antibiotics were ciprofloxacin, gentamicin, levofloxacin and imipenem (25%). Trimethoprim/sulfamethoxazole was resistant to all gram negative isolates.

DISCUSSION

Dacryocystitis is one of the most common diseases of the eye. It is an important cause of ocular morbidity both in children and adult.[1] Hence it requires special attention regarding the initiation of appropriate treatment at the earliest. In the present study, 59 clinically diagnosed cases of dacryocystitis attending ophthalmology out-door department in a tertiary care teaching hospital, Kolkata were studied. The pattern of relative incidence of various factors varies in different studies.

The present study shows that the infection is common in females 44(74.58%) as compared to males 15(25.42%). The male to female ratio was 1:2.93.In congenital dacryocystitis, females were 6 and males were 3 and ratio of 1:0.5 which correlates with the study of Kuchar A *et al*[8] i.e., 1:0.74. Males were predominant in congenital dacryocystitis in some studies like Ghose *et al*[1] female and male ratio 1:2 and Usha *et al*[7] female and male ratio is 1:1.2. In acquired dacryocystitis, female to male ratio in the present study was 2.92:1 which correlates with the studies of Badhu *et al*[9] 2.1:1, Machin *et al*[10] 2.7:1 and Morgan *et al*[5] 2:1. Brook *et al* [4] observed males more than females (female: male = 0.63:1). The predilection in females may be due to the smaller nasolacrimal canal diameter in females than men and hormonal factors. Most of the females come from middle and lower income group working with wood and dried cow dung for cooking which gives away lot of smoke particles which settled down in conjunctival sac and enter nasolacrimal duct through tears and block nasolacrimal duct. Kajal artificially prepared in house may have been contaminated with organisms, when applied on the margin of the lids may infect the lacrimal sac. Females blow the nose infrequently when compared to the males, which causes stagnation of nasolacrimal duct secretions and leading to infection. Apart from the special case in dacryocystitis in the new born which depends on developmental anomalies, the disease affects preferentially adults over 40 years of age, being relatively rare in children and adolescents, the highest incidence being in fifth decade but it also occurs in advanced age. In this study the highest occurrence was in the age group 46-60 years (32.20%). This correlates well within the limits of study conducted by Chaudhry *et al*[11] and by Hartikainen *et al*[12]. Excessive secretion of tears leading to stagnation with a tendency to atony of the sac, thus resulting eventually in chronic irritation, inflammation and weakening of resistance to organism attack. Females of low socio-economic class working in the houses are more exposed to smoke which leads to excessive secretion of tears and accumulation of small particles in the conjunctival sac.

In our study involvement of eye is mainly unilateral (83.05%) either right or left and some bilateral (16.95%) cases. This correlates well with the study of Ghose *et al*.,[1] (90%:10%), Sun *et al*.,[13] (90.1%: 9.9%) and Machin *et al*.,[10] (91.3%: 8.7%). Noda *et al*.,[14] noticed 52.3% of unilateral dacryocystitis and 47.7% of bilateral dacryocystitis. Brook *et al*.,[4] study showed only unilateral cases and no bilateral cases. There is a relatively high incidence of disease on left side (40%) as compared to right side (32%). This correlates well with Brook *et al*.,[4] studies in which left lacrimal sac was involved in 36 patients (58%). In Usha *et al*.,[7] study, right lacrimal sac was involved in 76(40%) patients and left lacrimal sac was infected in 60(33%). In general the disease has predilection to left side especially in females because of narrow bony canal. In many instances, the nasolacrimal duct and lacrimal fossa formed a greater angle on the right side than the left side. Chronic dacryocystitis was the most frequently encountered clinical type 33(55.93%) and acute dacryocystitis was 18(30.81%) in the present study. Congenital dacryocystitis encountered was (13.56%). In Campolattaro *et al*[15] study, chronic dacryocystitis was 36(67%) and acute dacryocystitis was 18(33%). This is probably because acute dacryocystitis invariably leads to chronic dacryocystitis.

In the present study the main presenting feature is epiphora with mucous or mucopurulent discharge (57.63%) followed by epiphora with mucous or mucopurulent discharge and swelling, redness (28.81%). Least frequent complaint in this study is epiphora only (13.56%). Whereas the study conducted by Hartikainen *et al*[12] which showed epiphora in 52.7% and purulent discharge in 47.4%. In a study by Machin *et al*[10] showed mucopurulent discharge in 26.4%, mucocele in 4.8% and epiphora in 52%. Study by Shiva reddy *et al*[16] showed epiphora in 80%, purulent discharge in 75% and mucocele or swelling in 25%. Kuchar *et al*[8] study showed more cases with purulent discharge (68.1%) and with epiphora (31.9%). Epiphora is the commonest nature of discharge probably because it is the mode of presentation of many causes of dacryocystitis.

In this study out of 59 cases of dacryocystitis, 9 bacterial isolates were obtained. Single organisms were isolated in 15 (23.42%) of the cases and mixed organisms in 1 (1.69%). Whereas studies of Kundu *et al*[2](82.5% and 10.5%), Sainju *et al*[17] (81.82% and 18.18%) and Usha *et al* (88.3% and 11.7%). Hartikainen *et al*[12] had a higher percentage of mixed organisms (48%) than other studies. Chaudry *et al*[11] study showed multiple organisms (66.1%) more than single organisms (33.9%) in culture which is probably related to the duration of the disease.

Bacterial isolates have been changing from time to time and from place to place. Out of 9 isolates cultured from 59 samples, gram-positive organisms were 4(45%) and gram-negative organisms were 5(55%). The study of Bareja U *et al*[18] shows out of 90 isolates *Streptococcus pneumoniae* were 33(28.9%) and *Pseudomonas aeruginosa* were 5(4.4%). Studies by Kuchar *et al*[8] and Usha *et al*[7] showed *Streptococcus pneumoniae* (36.4% and 32.7%) and *Haemophilus influenzae* (19.2% and 31.3%) respectively. In acquired dacryocystitis, most common gram-negative isolates are *Pseudomonas aeruginosa*. This correlates with studies of Briscoe *et al*[19] (13% and 22%), Sainju *et al*[16] (34.1% and 7.6%) and Brook *et al*[4] (15.95% and 5.3%). In other studies like Shamna *et al*[20] *Streptococcus pneumonia* was common (42%) followed by *Haemophilus influenzae* and *Acinetobacter* (8%), whereas Hartikainen *et al*[12] stated that *Staphylococcus epidermidis* (26.9%) was the commonest followed by *Haemophilus influenza* (3.8%).

The antimicrobial sensitivity pattern varies from community to community. This is because of emergence of resistant strains as a result of indiscriminate use of antibiotics. The gram-positive isolates were most sensitive to vancomycin, oxacillin, linezolid and clindamycin (100%), followed by trimethoprim/sulfamethoxazole (66.6%) and gentamicin (33.3%). Ciprofloxacin and levofloxacin were resistant to all gram positive isolates. The gram-negative organisms were most sensitive to cefepime (75%), followed by amikacin, ceftazidime and piperacilin (50%). The least sensitive antibiotics were ciprofloxacin, gentamicin, levofloxacin and imipenem (25%). Trimethoprim/sulfamethoxazole was resistant to all gram negative isolates. In a study by Kuchar *et al*.,[8] of congenital dacryocystitis, ofloxacin and tetracycline turned out to be the most effective single agents (84.9%) to all gram-positive and gram-negative isolates. These were followed by chloramphenicol (83.6%), bacitracin and ciprofloxacin (61.6%) and norfloxacin (60.3%). Ghose *et al*.,[1] showed that the most effective single antibiotic against all organisms was tobramycin (100%), followed by gentamicin (97%) and vancomycin (97%). Briscoe *et al*.,[19] revealed that gram-negative isolates were sensitive to ceftazidime (95%), ciprofloxacin (86%) and cefuroxime (50%), with a sensitivity of less than 30% to cefalexin and ampicillin. *Pseudomonas aeruginosa* were sensitive to ceftazidime (100%), ciprofloxacin (86%), ampicillin (20%) and cephalexin (14%). Sun *et al*.,[13] studies sensitivity tests revealed that levo-ofloxacin and amikacin were the most effective antibiotics. In Usha *et al*.,[7] studied that gram-positive organisms exhibited a high rate of sensitivity to chloramphenicol, vancomycin and ofloxacin.

CONCLUSION

Chronic dacryocystitis is the most common mode of dacryocystitis than acute dacryocystitis and majority of patients shown serous discharge. Number of female patients of middle age and above had higher cases of dacryocystitis than men. Left eye was more infected than right eye. *Pseudomonas aeruginosa* is commonest

organism isolated in congenital as well as in acute dacryocystitis. In acute form infection may come from pond bathing and poor hygiene whereas *Staphylococcus aureus* is more common in chronic form. Most effective antibiotics for gram-positive bacteria were vancomycin, oxacillin, linezolid and clindamycin, followed by gentamicin and trimethoprim/sulfamethoxazole. On the other hand cefepime followed by amikacin, ceftazidime and piperacilin were promising against gram-negative bacteria. Significant association was found between the sex and nature of discharge, sex and chronicity of disease in dacryocystitis but not in the age and sex. Most of the chronic dacryocystitis cases are asymptomatic and in few cases where organisms can be isolated most show multiple drug resistance. Further research is needed to reveal the unknown facts of chronic dacryocystitis.

REFFERENCES

1. Ghose S, Nayak N, Satpathy G et al. Current Microbial Correlates of the Eye and Nose in Dacryocystitis – Their Clinical Significance. AIOC Proceedings, 2005; 437-439.
2. Kundu PK et al. Bacteiological profile in chronic dacryocystitis. J Indian Med Assoc, 2006; 104(7): 398-400.
3. Duke Elder S, Cook C. Diseases of the lacrimal passages. In: Duke-Elder S. Eds. System of Ophthalmology, Vol XIII, Part II. St. Louis, CV Mosby, 1974: 675–724.
4. Brook I, Frazier EH. Aerobic & Anaerobic Microbiology of Dacryocystitis. Am J Opthalmol, 1998; 125(4): 552–554.
5. Morgan S, Austin M, Whitter H. The treatment of acute dacryocystitis using laser assisted endonasal dacryocystorhinostomy. British Journal of Ophthalmology, 2004; 88: 139-141.
6. McEwen, Donna R. Surgical Treatment of Dacryocystitis: AORN J, 1997; 66(2): 268-280.
7. Usha K et al. Spectrum and the Susceptibilities of Microbial Isolates in Cases of Congenital Nasolacrimal Duct Obstruction. JAAPOS, 2006; 10(5): 469-472.
8. Kuchar A, Lukas J, Steinkogler FJ. Bacteriology and antibiotic therapy in congenital nasolacrimal duct obstruction. Acta Ophthalmol Scand, 2000; 78: 694-698.
9. Badhu B et al. Epidemiology of chronic dacryocystitis and success rate of external dacryocystorhinostomy in Nepal. Orbit, 2005; 24(2): 79-82.
10. Machin SJ et al. Lacrimal duct obstruction treated with lacrimonasal stent. Arch Soc Esp Optalmol, 2003; 78(6): 315-318.
11. Chaudhry IA, Shamsi FA, Al-Rashed W. Bacteriology of chronic dacryocystitis in a tertiary eye care centre. Ophthal Plast Reconstr Surg, 2005; 21(3): 207–210.
12. Hartikainen J, Lehtonen OP, Saari KM. Bacteriology of lacrimal duct obstruction in adults. Br. J. Ophthalmol, 1997; 81: 37-40.
13. Sun X et al. Microbiological analysis of chronic dacryocystitis. Oph Phys Optics, 2005; 25(3): 261-263.
14. Noda S, Hayasaka S, Setogawa T. Congenital nasolacrimal duct obstruction in Japanese infants: its incidence and treatment with massage. J Pediatr Ophthalmol Strabismus, 1991; 28(1): 20-22.
15. Campolattaro BN, Lueder GT, Tychsen L. Spectrum of pediatric dacryocystitis: medical and surgical management of 54 cases. J Pediatr Ophthalmol Strabismus, 1997; 34(3): 143-153.
16. Shiva Reddy P. Bhaskara Reddy D. Dacryocystitis – A clinico pathological study. J Indian Med Assoc, 1955; 24: 413–416.
17. Sainju R, Franzco AA, Shrestha MK, Ruit S. Microbiology of dacryocystitis among adults population in southern Australia. Nepal Med Coll J, 2005; 7(1): 18-20.
18. Bareja U, Ghore S. Clinicobacteriological Correlates of Congenital Dacryocystitis. Ind J Opthal, 1990; 38(2): 66–69.
19. Sun X et al. Microbiological analysis of chronic dacryocystitis. Oph Phys Optics, 2005; 25(3): 261-263.
20. Shamna KV et al. Clinicopathological correlation in chronic dacryocystitis. AIOC PROCEEDINGS, 2003; 533-534.

Oxidative Stress in *Entamoeba histolytica*

14

Somasri Dam, Pinaki Biswas, and Raktim Ghosh

Abstract

Entamoeba histolytica is a human pathogen, responsible for invasive amoebiasis and dysentery. This chapter aims to describe the effect of various stresses especially oxidative and nitrosative stress on this organism. This parasite is subjected to several types of stress throughout its life cycle and also during the invasion of human tissues as a result of host's response to the infection. For successful infection, it must produce an adaptive response against host defense mechanisms. *E. histolytica* is microaerophilic, but during tissue invasion, it is exposed to high oxygen content in well-perfused tissues. This parasite has its own antioxidant strategy to protect itself against reactive oxygen and nitrogen species generated by both host and parasite. *E. histolytica* doesn't have most of the antioxidant defense mechanisms such as glutathione peroxidase, glutathione reductase, and catalase. Instead, it manages the antioxidant components from engulfed bacteria and red blood cells. L-cysteine takes a major role to protect the trophozoites of *E. histolytica* from oxidative stress and nitrosative stress as the parasite lacks glutathione, a major thiol in eukaryotes. During oxidative stress caused by H_2O_2, 286 genes have been found to be upregulated in *E. histolytica* HM1: IMSS. In response to environmental stresses like glucose starvation, serum starvation, iron starvation, heat shock, and UV irradiation, several responsible genes are either downregulated or upregulated in this pathogen.

Keywords

Entamoeba histolytica · Oxidative stress · Nitrosative stress · Starvation · L-Cysteine

S. Dam (✉) · P. Biswas · R. Ghosh
Department of Microbiology, University of Burdwan, Burdwan, West Bengal, India
e-mail: dam_somasri@rediffmail.com

S. Chakraborti et al. (eds.), *Oxidative Stress in Microbial Diseases*,
https://doi.org/10.1007/978-981-13-8763-0_14

Abbreviations

ALDO	Aldolase
Eh	*Entamoeba histolytica*
GAPDH	Glyceraldehyde 3-P dehydrogenase
HK	Hexokinase
HPI	Hexose phosphate isomerase
ORP	Oxygen reduction pathway
UDP-GPP	UDP-glucose pyrophosphorylase
PFK	Phosphofructokinase
TPI	Triose-phosphate isomerase
PGK	Phosphoglycerate kinase
PGAM	Phosphoglycerate mutase
ENO	Enolase
PPDK	Pyruvate phosphate dikinase
PK	Pyruvate kinase
ADHE	Bifunctional aldehyde/alcohol dehydrogenase
AcCoAS	ADP-forming acetyl-CoA synthetase
GK	Glycerol kinase
GPP	Glycerol 3-phosphate phosphatase
PFOR	Pyruvate:ferredoxin oxidoreductase
Fd(ox) and Fd(red)	Oxidized and reduced ferredoxin
NO	NADPH-dependent oxidoreductase
FDP	Flavodiiron protein
p34	34-kDa NADPH:flavin oxidoreductase
FeSOD	Iron-containing dismutase
TrxR(ox) and TrxR(red)	Oxidized and reduced thioredoxin reductase
Trx	Thioredoxin
Rbr(ox) and Rb(red)	Oxidized and reduced rubrerythrin
NROR	NAD(P)H-dependent rubredoxin reductase
Prx(ox) and Prx(red)	Oxidized and reduced peroxiredoxin
ISF	Iron-sulfur flavoprotein
HCP	hybrid cluster protein
Eh34/p34	Flavin oxidoreductase
Trans-PMET	Transplasma membrane electron transport
TPQ-7	Thermoplasmaquinone-7
PNT	Pyridine nucleotide transhydrogenase
CoA	Coenzyme A
ATP	Adenosine triphosphate
$NAD(P)^+$	Oxidized nicotinamide adenine dinucleotide (phosphate)
NAD(P)H	Reduced nicotinamide adenine dinucleotide (phosphate)

14.1 Introduction

Entamoeba histolytica causes amoebic colitis and liver abscess worldwide. This tissue-lysing amoeba is the causative agent for amoebiasis which persists as a global health problem leading to 50 million clinical cases and 40,000–100,000 deaths annually [1]. Amoebiasis occurs worldwide and it is a major problem where poor sanitation causes contamination of drinking water and food with feces [1–4]. It is the second most lethal disease in the world caused by protozoan parasite after malaria [5]. Amoebic colitis was known to the ancients. The disease was first documented in a Sanskrit description as bloody mucoid diarrhea during 3000 BCE [6]. It took more than 2000 years to be invented. Amoeba was first identified as a reason of dysentery in 1875, when the St Petersburg physician Fedor Aleksandrovich Lösch identified the trophozoites of amoeba in the stool of a farmer with a fatal case of dysentery [3].

E. histolytica has high potential for invading and destroying the tissue in human colon causing hemorrhagic colitis. During residing in human gut, the parasite lives in the environment of reduced oxygen pressure. The production of reactive oxygen species (ROS) is an important component of the innate immune defense against microbial infections, including amoebiasis [7]. In this case, the parasite experiences high amount of exogenous ROS during tissue invasion of the host, which may lead to metabolic malfunctions. Several defense mechanisms including enzymatic and non-enzymatic components help to protect the pathogen against the oxidative stress.

14.2 Stress-Related Studies in *Entamoeba histolytica*

E. histolytica undergoes different types of environmental stresses during its life cycle. These can be classified mainly into seven categories, such as oxidative and nitrosative stress, glucose starvation, cysteine starvation, iron starvation, heat shock, and UV irradiation [8]. The parasite is challenged in host environment mostly due to the major fluctuations in oxygen level and glucose concentration level. The activation of innate immune response against *E. histolytica* directs to the production of ROS and NO by macrophages. This helps *E. histolytica* to become capable of adapting the oxidative stress [9]. Most of the eukaryotic organisms respond to environmental stress by reducing or switching off the protein synthesis process. The exception is synthesis of heat shock proteins and some transcription factors [10]. *E. histolytica* is not an exception. Table 14.1 summarizes the role of proteins and enteric bacteria during various stresses in this parasite. *E. histolytica* shows a specific heat shock response with overall reduction in gene transcription including the genes responsible for its virulence, such as galactose/N-acetylgalactosamine (Gal/GalNAc) lectin, certain cysteine proteinases, and a 20-kDa antigen [11]. Ultraviolet light produces cyclobutane pyrimidine dimers, oxidized bases, single-strand breaks, and also DNA double-strand breaks (DSB) [12, 13]. DSB is a critical injury to DNA, and it activates a complex network of proteins that may arrest cell cycle to enhance DNA repair mechanisms [14]. A cDNA microarray study on global

Table 14.1 *E. histolytica* proteins during various stresses

Type of stress	Protein involved	Summary of study	References
Heat shock Oxidative stress	Ehssp1	Stress condition upregulates the expression of polymorphic copies of Ehssp1, antigenic in invasive amoebiasis Extent of polymorphism differs between pathogenic and non-pathogenic strain	[130]
Oxidative stress.	Eh29 HSP70A2 EhSOD EhCP5 G protein Peptidylprolyl isomerase	In response to oxidative stress, several genes are upregulated in a time-dependent manner to protect *E. histolytica* during invasion	[43]
Oxidative stress.	Eh29	29-kDa surface antigen, exhibits protective antioxidant activities Survival and pathogenesis of *E. histolytica* through invasion increase with increased expression of Eh29	[58]
Oxidative stress Nitrosative stress	Heat-shock proteins Ubiquitin-conjugating enzymes Protein kinases and small GTPases	During oxidative and nitrosative stress, a large set of genes are either upregulated or downregulated and their expression may differ in pathogenic and non-pathogenic strains of *E. histolytica*	[44]
Oxidative stress	EhPFOR EhADH2	Trophozoites under oxidative stress modify their energy metabolism by regulating the steps of glycolysis	[48]
Oxidative stress Nitrosative stress	EhFdp1	*E. histolytica* genome contains four genes encoding flavodiiron proteins which are likely to be acquired by horizontal gene transfer from prokaryotes EhFdp1 is cytoplasmic, having specific and high oxygen reductase activity but poor nitric oxide reductase activity	[131]
Oxidative stress Nitrosative stress	EhTRXR.	EhTRXR catalyzes the NAD(P)H-dependent reduction of thioredoxins and S-nitrosothiols	[132]
Oxidative stress Nitrosative stress	EhSIAF EhPTPA	In oxidative and nitrosative stressed condition, *E. histolytica* shows higher transcription level of EhSIAF and EhPTPA EhSIAF and EhPTPA are responsible for increasing adherence to the host cells and reduction in motility	[77]
Oxidative stress	H_2O_2-regulatory motif (HRM) binding protein	Overexpression of the transcription factor, HRM-binding protein increases the virulence potential in *E. histolytica* This is a special transcription factor controlling the transcriptional regulatory network in response to oxidative stress induced by hydrogen peroxide	[133]

(continued)

Table 14.1 (continued)

Type of stress	Protein involved	Summary of study	References
Oxidative stress	EhPFOR EhPrx EhFDP EhHSP70	Virulent strain of *Entamoeba* differs from non-virulent strains in gene expression level of several proteins related to oxidative stress HSP70 protects *E. histolytica* from oxidative damage in O_2 exposure and may contribute to its virulence	[134]
Oxidative stress	Arginase Gal/GalNAc	A total, 154 number of oxidized proteins were detected which are functionally associated with antioxidant activity Oxidation of Gal/GalNAc has inhibitory effect on adherence of *E. histolytica* trophozoites to host cells Novel function of arginase in protection of parasite against oxidative stress has been identified	[17]
Oxidative stress	EhTrx EhFDP1 EhRbr EhPrx EhTrxR	Proteins of thiol-based redox system counteract with oxidative and nitrosative stress and maintain intracellular redox potential during invasion, colonization, and disease progression Proteins of thiol-based redox system can be used as a suitable drug target for disruption of redox balance in parasite	[61]
Oxidative stress	Serine-rich *Entamoeba histolytica* protein (SREHP) Eh29 Gal/GalNAc lectin	In silico analysis of protein related to stress response in *E. histolytica* can serve future prospect in developing of diagnostic markers, drug design, and vaccine research	[135]
Oxidative stress ER stress Thermal stress	EhPDI	Stressful condition inhibits EhPDI activity resulting in unfolding, aggregation, and inability to assist the refolding of proteins	[136]
Oxidative stress	Thioredoxin Peroxiredoxin Nitroreductase Oxidoreductase	Enteric bacteria except probiotics protect the parasite from oxidative stress	[83]

transcriptional response to the DNA damage of *E. histolytica* showed that most gene regulation in response to UV-C irradiation is operating at post-translational level. Importantly, several genes encoding Fe–S clusters containing proteins involved in stress adaptation were found to be upregulated and some genes encoding cytoskeleton proteins were downregulated upon UV exposure. This is probably due to the fact that *E. histolytica* actin dynamics is arrested to permit proper repairing of DNA damage caused by UV-C irradiation [15].

14.2.1 Oxidative Stress

Among the parasitic protozoa, *Entamoeba histolytica* is unique because of its in vitro nutritional requirements and in vivo pathogenicity mechanisms. Until now, very little is known regarding molecular factors and physicochemical conditions that regulate the growth, establishment, and successful invasion of this parasite in the host. It can be grown in vitro under the condition of low oxygen concentration and it is susceptible to metabolically produced toxic oxygen derivatives and ROS. The parasite may also consume low amount of oxygen and therefore produce some toxic reactive oxygen derivatives. *E. histolytica* lacks catalase, glutathione reductase, and glutathione peroxidase, the major defense mechanisms in other aerotolerant cells. For this reason, *E. histolytica* has evolved itself with some alternative approaches. It phagocytoses bacteria during the commensal phase, and during invasive phase, it consumes red blood cells (RBCs). These engulfed bacteria or RBCs, through their intact form or antioxidant component form, detoxify the ROS produced in their intracellular environment during invasion phase [16]. In a study, 154 number of proteins have been found to be oxidized in oxidatively stressed trophozoites of *E. histolytica* in resin-assisted capture coupled to mass spectrometric analysis [17]. Unlike many organisms, *E. histolytica* lacks glutathione which plays as major thiol in most eukaryotes. In this parasite, L-cysteine works as a principal low molecular weight thiol [18]. Growth medium lacking L-cysteine elevates intercellular ROS level by more than threefold, implicating the significance of this amino acid in the antioxidant defense against the oxidative stress [19]. Apart from this, L-cysteine protects the trophozoites of *E. histolytica* from oxidative shock generated by treatment with the drug metronidazole [20]. L-cysteine can be obtained either through a de novo synthesis pathway or via uptake from extracellular environment. The de novo synthesis is carried out in two steps catalyzed by serine acetyltransferase and cysteine synthetase [21, 22]. Experimental data showed that internal concentration of L-cysteine is almost undetectable when the trophozoites are cultured in a medium devoid of cysteine. This clearly implies that the de novo synthesis pathway itself is not sufficient to maintain intracellular concentration up to the mark and it mostly depends on external uptake. During nitrosative stress, the trophozoites of *E. histolytica* overexpress cysteine synthetase to satisfy the increased amino acid demand. Fig. 14.1 describes the various antioxidant pathways operating in *E. histolytica*.

14.2.2 Glucose Starvation

E. histolytica faces glucose starvation in human colon because the available glucose is very low due to high absorptive capacity of the glucose transporters in small intestine [23–25]. In response to glucose starvation, several genes related to glycolysis are downregulated, and the genes involved in degradation of stored carbohydrates are upregulated. From the proteomics and transcriptomics study, it has been found that mainly three genes/proteins get upregulated, namely, Gal/GalNAc lectin,

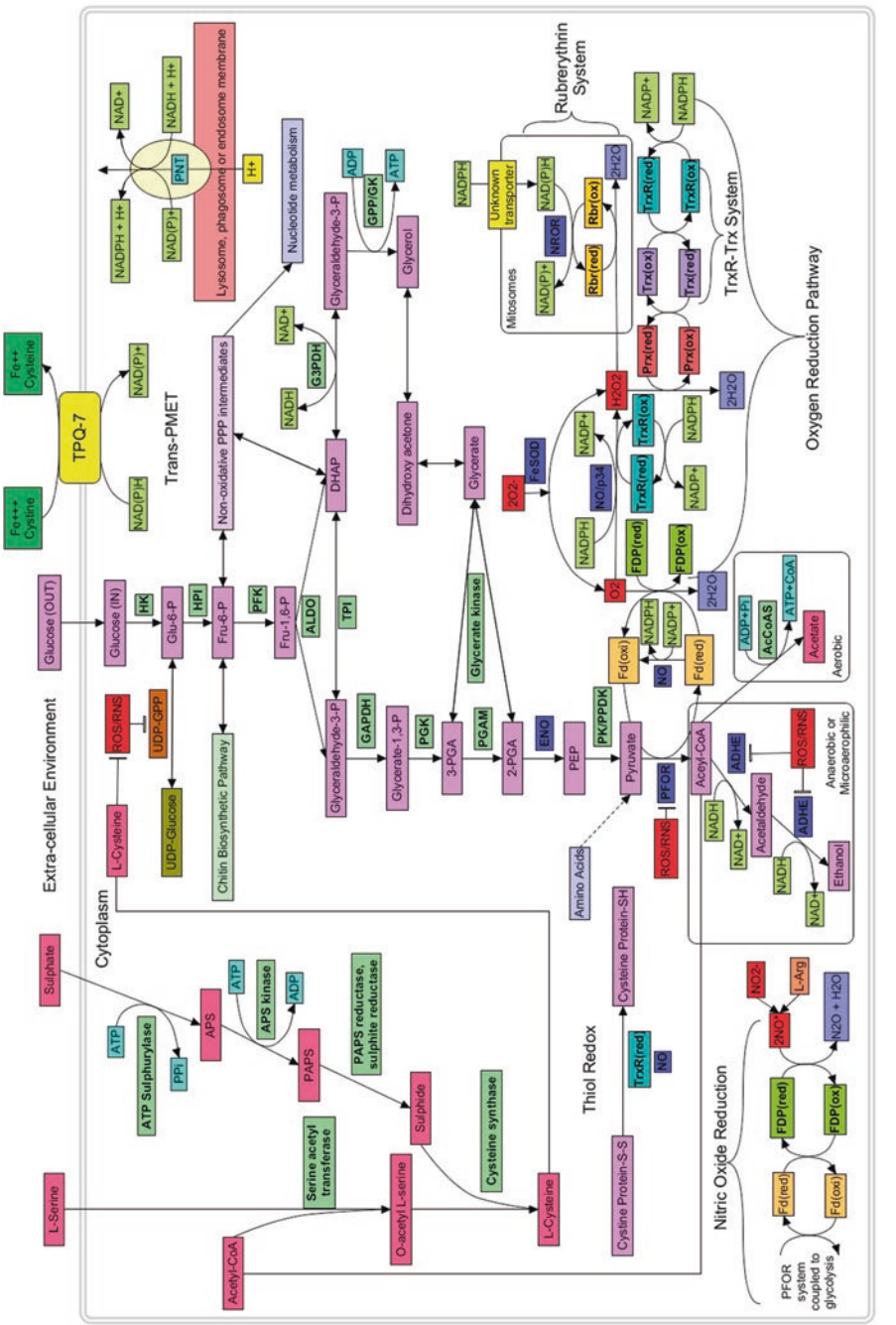

Fig. 14.1 Schematic representation of antioxidant pathways in *Entamoeba histolytica*

dihydropyrimidine dehydrogenase (DPD), and MGL-1 [26, 27]. DPD is involved in the degradation of pyrimidine. So, its increased expression in *E. histolytica* during glucose starvation may be due to the energy production by degradation of pyrimidines [28, 29]. Another carbon source to catch up the needs for energy is to break down the colonic mucin by β-amylase [30]. Glucose starvation enhances virulence property by upregulation of virulence factors such as Gal/GalNAc lectins and a cysteine protease, EhCP-A4, that helps the parasite to invade host by destroying the intracellular matrix [26]. Glucose starvation stimulates epigenetic regulation by building up the shuttling of glycolytic enzyme enolase in the nucleus and inhibition of Ehmeth [27].

14.2.3 Iron Starvation

Iron is one of the essential elements used for growth of *E. histolytica*. Ferric ammonium citrate is used as iron source in medium preparation for maintaining the axenic culture of *E. histolytica* in laboratory condition [31]. When present in a host, iron demand is satisfied by scavenging iron from host's normal gut flora and also from the iron-containing proteins of host such as hemoglobin and ferratin [32]. NifS, NifU, and rubrerythrin form the iron-sulfur cluster in this parasite [33, 34]. These are essential for proper enzymatic activity of superoxide dismutase, alcohol dehydrogenase 2, and ferredoxin [35]. In vitro experiments showed that low iron concentration significantly decreases the adherence property and cytopathic activity in the parasite [36, 37]. Thus, iron is exclusively and directly linked to its pathogenicity and no other cationic salts are known for this effect [37]. It is evident from transcriptome analysis that when grown in absence of iron, the trophozoites show an increase in transcriptional activity of some proteins, such as cysteine proteinases (CP-EHI_01850, CP-A5, and CP-A7), translation elongation factors, and ribosomal proteins. Stress signal from iron deprivation upregulates the expression of androgen-inducible Gene 1 (AIG1), acyl-CoA synthetase, ComEC protein, and NADPH-dependent oxidoreductase (EhNO2) [38]. Three genes of AIG1 family, EHI_195260, EHI_115160, and EHI_022500, are highly expressed during liver abscess in cell line study signifying its connection with virulence [39]. Reduction from cystine to cysteine is done by EhNO2 to meet the cellular level of cysteine for various functions. EhNO2 reduces the amoebiasis drug, metronidazole, which becomes activated and generates toxic reactive species [40]. During iron starvation of *E. histolytica*, there is an increased gene expression of different transport family proteins such as ABC family of transport proteins, P-glycoprotein-5, and major family transporters to increase the influx of iron from different sources [38, 41].

14.3 Genes Upregulated and Downregulated During Oxidative and Nitrosative Stress

E. histolytica should have different defense strategies to cope with the major stresses caused by cytotoxic reactive species. ROS and RNS are produced during the tissue invasion process by the parasite as it moves from anaerobic colonic lumen to oxygen-rich colonic tissues [3]. ROS and RNS target several cellular proteins, nucleic acids, and lipids [42].

Upon exposure to high oxidative and nitrosative stresses and during the transition from anaerobic to aerobic metabolism, *E. histolytica* upregulates several genes [43–45]. Some of the genes for detoxification of ROS and RNS have been acquired probably from prokaryotes by horizontal gene transfer mechanism [46, 47]. Whole genome microarray revealed that a considerable number of genes are upregulated during oxidative stress in both pathogenic strain of HM1: IMSS (ATCC 30459) and non-pathogenic strain Rahman (ATCC 30886) [44]. However, non-pathogenic strain *E. histolytica* Rahman showed relatively lower number of transcriptional changes. In *E. histolytica* HM1: IMSS, 286 genes were upregulated upon exposure to H_2O_2, whereas for nitrosative stress, the number was 1036 genes. 164 genes overlapped in both stress conditions. 102 genes in total were found to be downregulated due to oxidative stress. Although most of these genes were hypothetical proteins, Rab family GTPase (XM_645246), cyclin (XM_647175), and mitotic inducer phosphatase (XM_644512) were among the known proteins which were downregulated by oxidative stress [44].

14.4 Role of Cellular Proteins

14.4.1 Pyruvate: Ferredoxin Oxidoreductase (EhPFOR)

Controlling steps of energy metabolism in *E. histolytica* are affected by oxidative stress [48]. The organism has neither tricarboxylic acid cycle nor oxidative phosphorylation steps. ATPs are mainly generated by glycolysis with pyruvate as end product. Pyruvate is decarboxylated oxidatively by pyruvate: ferredoxin oxidoreductase (EhPFOR; E.C 1.2.7.1) to acetyl-CoA. In microaerophilic condition, acetyl-CoA is further reduced to acetaldehyde and ethanol, catalyzed by a bifunctional NADH-dependent aldehyde-alcohol dehydrogenase (EhADH2), whereas in aerobic condition, it produces ethanol and acetate by EhADH2 and ADP-forming acetyl-CoA synthetase (AcCoAS, E.C 6.2.13) [49–52]. A characteristic feature of anaerobic protozoan parasites like *Entamoeba* [51], *Giardia* [53], and *Trichomonas* [54] is the absence of pyruvate dehydrogenase complex which converts pyruvate to acetyl-CoA. PFOR connects glycolysis with carbohydrate fermentation. EhPFOR can be detected in plasma membrane and cytoplasmic structures of the trophozoites [48]. Interestingly, it has high preference for pyruvate over other oxoacids [48]. Enzymatic activities of EhPFOR and EhADH2 are susceptible to reactive oxygen species.

14.4.2 Thiol-Dependent Peroxidase/Peroxiredoxin (Eh29/EhPrx)

E. histolytica lacks catalase and glutathione reductase machinery to deal with oxidative stress, but it has a cysteine-rich thiol-dependent peroxiredoxin, EhPrx, or Eh29, a surface antigen located in its outer membrane [55]. This 29-kDa thiol-dependent peroxiredoxin of *E. histolytica* is homologous to alkyl hydroperoxide C-22 protein, AhpC of *Salmonella enterica* serovar typhimurium, and a thiol-specific antioxidant protein of *Saccharomyces cerevisiae* [56]. Under oxidative stress, this protein helps to detoxify the system by reducing peroxides and peroxynitrites [57]. As a membrane-bound peroxyredoxin, Eh29 removes H_2O_2 generated in metabolic processes [58]. A conserved cysteine residue in this 29-kDa protein participates in a cyclic process of peroxide-dependent oxidation and thiol-dependent reduction to protect from H_2O_2 generated by oxidative stress both from internal and external sources [57, 59]. During tissue adherence and invasion, it binds to cytosolic domain of galactose/N-acetylgalactosamine lectin present in surface membrane which carries the signal to counteract the parasite from oxidative attack by the activated host phagocytic cells and epithelial cells, promoting a successful invasion [58, 60, 61].

14.4.3 Flavodiiron Protein (EhFDP1)

Flavodiiron proteins (FDPs) are fundamental constituents of a wide variety of detoxifying enzyme families that work as oxygen and/or nitric oxide reductases [62–64]. Substrate specificity of FDPs is still not clear. Some are selective towards oxygen, a few proteins are selective to nitric oxide, and others have equal selectivity for both. Most prokaryotic anaerobes have FDP-encoding genes and a few anaerobic protozoa contain single or multiple homologs of FDP in their genome. In *E. histolytica* genome, four genes have been identified encoding FDPs [65], whereas *Giardia intestinalis* has one and *Trichomonas vaginalis* has four homologs of FDP. In protozoa, FDPs mainly act as oxygen reductases [47, 66–68]. These genes are probably acquired from prokaryotes via lateral gene transfer [46, 47].

14.4.4 G Protein

G proteins along with other oxidative stress-related proteins is overexpressed during exposure to highly oxygenated environment compared to normally grown *E. histolytica* in axenic culture. A series of signal transduction cascades function during the oxidative stress of this parasite that control the activity of related transcription factors. G protein regulates expression of several genes which are necessary to maintain normal cellular functions to overcome oxidative stress [43].

14.4.5 DNA Methyl Transferase (Ehmeth)

Nitric oxide (NO), released by natural killer cells, activated macrophages, and other phagocytic cells, has a crucial role in host's defense mechanism against pathogens by inhibiting protein synthesis machinery. The responsible factors for this inhibitory activity include NO-mediated cleavage of 18S and 28S rRNA [69] and NO-induced phosphorylation of eukaryotic initiation factor eIF-2α [70]. To overcome the deleterious effect of NO, *E. histolytica* increases the expression of Ehmeth, the cytosine-5-methyltransferase from Dnmt2 family. Experimental data suggests that Ehmeth has a strong connection with Ehmeth-mediated tRNA methylation and process of protein synthesis in this parasite under nitrosative stress [71]. Methylation at 5′-cytosine probably increases tRNA stability and upregulation of 40S and 60S ribosomal proteins maintains the level of protein synthesis. Nitrosative stress-mediated epigenetic regulation of gene expression is also possible [72]. S-Nitrosylation in cysteine residues 228–229 of Ehmeth negatively regulates the activity of Dnmt2 domain and prevents the formation of Ehmeth-enolase complex [73]. In complex form, enolase suppresses the activity of tRNA methylation of Ehmeth. tRNA stability by methylation does not occur in normal or unstressed condition and, therefore, Ehmeth largely remains in Ehmeth-enolase complex in this parasite. During nitrosative stress, S-nitrosylation in cysteine residues inhibits the complex formation and invokes the stress response for survival [71]. *E. histolytica* takes typical strategy like downregulation of protein synthesis to cease energy wasting and building up the intracellular toxicity by production of damaged or misfolded proteins [11, 74].

14.4.6 N-Acetyl Ornithine Deacetylase (EhNAOD)

During acute nitrosative stress, the expression of various redox proteins is increased in the trophozoites of *E. histolytica* [45]. The transcriptome study (RNA-seq) of *E. histolytica* treated with NO donor drug S-nitrosoglutathione (GSNO) shows upregulation of 208 genes, including N-acetyl ornithine deacetylase (EhNAOD, XP_649738.2, Pathema Id: EHI_114340). The trophozoites overexpressing glyceraldehyde 3-phosphate dehydrogenase are more sensitive to nitrosative stress than the control, and EhNAOD helps the parasite to neutralize the detrimental effect of glyceraldehyde 3-phosphate dehydrogenase during nitrosative stress [75]. *E. histolytica* depends on its dynamic actin-made cytoskeleton to move within different compartments of human body [76]. The genes which are associated with actin family cytoskeletal proteins are found to be upregulated during the adaptation of *E. histolytica* to nitrosative stress (Shahi et al. 2016b). The cysteine residues of actin are susceptible to oxidation.

14.4.7 Stress-Induced Adhesion Factor (EhSIAF), Phospholipid Transporting P-Type ATPase/Flippase (EhPTPA), and Arginase

A stress-induced adhesion factor (EhSIAF, XP_649092.1) and a phospholipid transporting P-type ATPase/flippase (EhPTPA, XP_653689.1) of *E. histolytica* are among the responsive genes against oxidative and nitrosative stress [44]. Overexpression of these two proteins enhances the survival of parasite under oxidative stress [77]. From transwell motility assay, it has been found that motility of trophozoites is reduced significantly due to the overexpression of EhSIAF and EhPTPA suggesting a boost in adherence property of the parasite [77]. Conversion of L-arginine to L-ornithine by enzymatic activity is an important source of L-ornithine for this parasite. Ornithine is required in the synthesis of polyamines, and these polyamines have protective role against nitrosative and oxidative stress. Arginase activity is very much essential for *E. histolytica*'s resistance to nitrosative stress [78] and oxidative stress [17]. Importantly, arginase activity is highly inhibited during oxidative stress of *E. histolytica* trophozoites, and arginase-overexpressing *E. histolytica* trophozoites are more resistant to the oxidative stress than control.

14.5 Effect of Enteric Bacteria on the Oxidative Stress Response

The human parasite *E. histolytica* lives in large intestine with many other microorganisms. *E. histolytica* can feed on bacteria and its pathogenicity may also depend on the microbiota present in the intestine [79]. The bacteria with appropriate recognition molecules are selectively ingested by the parasite [16, 80]. Presence of some bacteria may help the growth and pathogenesis of *E. histolytica*, whereas the presences of some filamentous bacteria are harmful for this parasite [79, 81, 82]. In amoebiasis, acute inflammation occurs during which ROS and RNS are released as a result of host immune response. This anaerobic parasite must be able to fight this oxidative stress to establish its pathogenicity. The study of *E. histolytica* transcriptome induced by oxidative stress and live *Enterobacteriaceae* reveals that *E. coli*, *Salmonella enterica* (an enteropathogen often found as co-infections with *E. histolytica*), and *Enterococcus faecalis* (present in human microbiota) protect *E. histolytica* against oxidative stress but not *Lactobacillus acidophilus* (a popular probiotic) [83]. Pre-incubation of *E. histolytica* with this probiotic is associated with the non-protective response involving some signalling molecules like oxidoreductases, kinases, and regulators of small GTPases [83]. In response to oxidative stress, 1402 genes including trafficking factors and small Rab GTPases are strongly downregulated and 1169 genes including ribosomal proteins, translation factors, hydrolases, and peptidases are strongly upregulated. However, no change of expression for these genes was observed upon pre-incubation with live bacteria (*E. coli* O55). LRR

proteins of *E. histolytica* play an important role in response to the oxidative stress and live bacteria [83].

14.6 Effects of Stress on the Cellular Events of *E. histolytica*

14.6.1 Effect of Oxidative and Nitrosative Stress on Adherence and Motility

Adherence capacity of oxidatively stressed trophozoites of *E. histolytica* to the HeLa cell monolayer is remarkably less than that of the untreated trophozoites [75]. The Gal/GalNac lectin consists of a heavy subunit, Hgl (170 kDa), and a light subunit, Lgl (35/31 kDa). Hgl mediates *E. histolytica* adherence. Under oxidative stress of trophozoites, Hgl can be oxidized and this may be the reason for reduced adherence and low motility of this parasite [17]. Motility is necessary for survival [84, 85], expressing pathogenicity, and intracellular trafficking of virulence factors [86]. Motility of parasite depends on dynamic actin cytoskeleton and other associated proteins like ARP2/complex whose function is affected by oxidative stress and nitrosative stress [87, 88].

14.6.2 Effect of Oxidative and Nitrosative Stress on Metabolic Activity

Cellular dysfunction of organisms is caused by exposure to various ROS and RNS as they damage the structural and functional units of cells such as proteins, lipids, and DNA [89–91]. Oxidative stress may promote apoptosis in higher eukaryotes, and this happens in *E. histolytica* also [91–94]. Antioxidant enzymes and free radical scavengers build up the powerful mechanisms to defend the cells [95]. From microbial world to higher eukaryotic system, cells avoid the destructive consequences of oxidative stress by a global modification of antioxidants and other metabolic enzymes. Metabolic alterations play a very important role to counteract the adverse effects of oxidative stress [96]. *E. histolytica* trophozoites face challenges by ROS and RNS during the steps of tissue invasion, colonization, and extraintestinal propagation to establish infection [3, 97]. The common antioxidant detoxification systems are absent in *E. histolytica* [18, 65, 98], but the genome of *E. histolytica* is equipped with genes encoding rubrerythrin, peroxiredoxin, hybrid-cluster protein, superoxide dismutase, and flavodiiron proteins for detoxification of ROS and RNS [58, 64, 65]. In *E. histolytica*, pyridine nucleotide transhydrogenase synthesizes NADPH from NADH by utilizing the driving force of electrochemical proton gradient across the membrane [99, 100]. A detailed study on oxidative stress-mediated metabolomic changes in *E. histolytica* reveals that various glycolytic intermediates, such as glucose 6-phosphate, fructose 6-phosphate, and pyruvate, are accumulated in the parasite due to free radical-mediated inactivation of glycolysis-related enzymes [101–103]. *E. histolytica* may accumulate G 6-P, F 6-P, and DHAP

on experimentally created nitrosative stress and this can mediate apoptosis in this parasite [102, 103]. In *E. histolytica*, pentose phosphate pathway (PPP) is absent due to the lack of glucose 6-phosphate dehydrogenase (G6PD) and transaldolases [65], and most intermediates of the non-oxidative branch of PPP – erythrose 4-phosphate (E4-P), ribose 5-phosphate (ribose 5-P), ribulose 5-phosphate (ribulose 5-P), and sedoheptulose 7-phosphate (S7-P) – are therefore increased upon oxidative stress [101]. On the other hand, *E. histolytica* has an alternative non-oxidative hexose-pentose interconversion pathway which does not require transaldolases, but depends mainly on three enzymes: phosphofructokinase, transketolase, and aldolase [104]. Ribose 5-phosphate produced in this pathway can serve as the precursor of NAD, which is further used by NAD kinase to generate NADP [105]. Pyridine nucleotide trans-hydrogenase catalyzes the conversion of NADP to NADPH using electrochemical proton gradient [99].

Life cycle of *E. histolytica* can be observed in two distinct morphological forms: trophozoite form which is proliferative, non-infective, but pathogenic and cyst form which is dormant, non-pathogenic, but infective. Cyst surface is shielded with chitin-made cell wall [106, 107]. Oxidative stress activates chitin biosynthetic pathway by two influential intermediates N-acetylglucosamine 6-phosphate (GlcNAc 6-P) and N-acetylglucosamine 1-phosphate (GlcNAc 1-P). Oxidative stress serves as the environmental stimulus to trigger the production of glucosamine 6-phosphate isomerase, an enzyme that converts GlcNAc 6-P and GlcNAc 1-P, and thus cyst-like structures are formed in *E. histolytica* via encystation process [108]. Genome sequence of *E. histolytica* suggests that ATP can be generated from amino acid catabolism during energy crisis and glucose starvation [109].

Sulfur-containing amino acids and their derivatives are synthesized and degraded by unique pathways in *E. histolytica*. Oxidatively stressed trophozoites show increased production of S-methylcysteine from O-acetylserine and methanethiol in a time-dependent manner [22, 110]. Functional trans-sulfuration pathways are missing, but the parasite possesses methionine γ-lyase for the degradation of sulfur-containing amino acids [111–114]. Unique de novo methanethiol and sulfur (sulfide) assimilatory pathways for synthesis of S-methylcysteine and L-cysteine are present in *E. histolytica* [110–112]. NADPH-dependent oxidoreductase acts as cystine reductase to restore L-cysteine [40]. O-phosphoserine, a precursor of L-serine and L-cysteine, increases significantly during oxidative stress [111, 112]. Glycolytic enzymes are highly susceptible to inhibition by ROS [115, 116]. In *E. histolytica*, activities of PFOR, phosphoglycerate mutase, and NAD^+-dependent alcohol dehydrogenase (ADH) are decreased greatly by oxidative stress, whereas there is a comparative marginal decrease in activities of GAPDH, TPI, PGK, ENO, and PPDK. *E. histolytica* can make glycerol from glucose, similar to other protozoa like *T. vaginalis*, *Trypanosoma brucei*, and *Plasmodium falciparum* [117–119]. Glycerol functions as an efficient free radical scavenger and it may protect against oxidative stress. One of the alternative mechanisms is the conversion of glycerol to dihydroxyacetone by glycerol dehydrogenase or glyceraldehyde by glyceraldehyde reductases [101].

14.6.3 Stress Response and Non-coding RNA

Short noncoding regulatory RNAs are present in *E. histolytica* [120–123]. These have an influential role in various cellular processes [124, 125]. EhslncRNA, long non-coding RNA, helps *E. histolytica* cells to overcome stressful conditions [126]. Various stresses like serum starvation, oxygen, and heat stress increase the expression of EhslncRNA indicating its role as a general stress regulator [127]. A 3′-5′ exoribonuclease, EhRrp6, in *E. histolytica* is lost from nucleus in response to stress including heat, oxidative stress, and serum starvation [128].

14.7 Conclusion

E. histolytica has developed multiple mechanisms to adapt oxidative stress, nitrosative stress, glucose starvation, serum starvation, UV exposure, and iron starvation. To survive in harsh environment, it increases or decreases the expression of specific genes. Some of these are common in different stresses, whereas the regulation of some genes is stress specific. A high number of genes are upregulated or downregulated as instant response of the parasite to a particular stress, such as after treatment with H_2O_2 or dipropylenetriamine-NONOate [44]. Moreover, it has the ability to adapt to diverse stresses, and various proteins are involved in this adaptation (Table 14.1). Dihydropyrimidine dehydrogenase helps to adapt in low glucose environment [26] and N-acetyl ornithine deacetylase is involved to overcome nitrosative stress of *E. histolytica* [129]. The activity of PFOR and ADH2 is highly inhibited when *E. histolytica* is subjected to high oxidative stress [102]. During nitrosative stress, Ehmeth-mediated $tRNA^{Asp}$ methylation is crucial to maintain active protein synthesis [71]. In absence of glutathione system and catalase, human pathogen *E. histolytica* overcomes the oxidative stress during invasion into the host cells with the help of thioredoxin system, L-cysteine, Eh29, and other stress-responsive proteins (Table 14.1).

Acknowledgments The financial assistance from BRNS, DAE (Project No. 37 (1)/20/15/2014-BRNS), and CSIR (Project No. 27(0322)/17/EMR-II) is thankfully acknowledged.

Legend to Figure 14.1: *E. histolytica* insulates itself from O_2 exposure, ROS, and RNS primarily by different enzymatic and redox reactions. In glycolytic pathway, glucose is converted into pyruvate via a series of biochemical reactions. Eventually, pyruvate is converted to acetyl-CoA catalyzed by PFOR, which is susceptible for ROS and RNS. In anaerobic or microaerophilic condition, ADHE converts acetyl-CoA into ethanol, but during high oxygen exposure, it produces acetate, indicating that activity of ADHE is inhibited by ROS/RNS. ROS/RNS inhibits the enzyme UDP-GPP. L-cysteine protects the parasite against harmful consequences of ROS/RNS attack by shielding the enzymes to maintain their normal metabolic pathways. L-cysteine can be synthesized in a de novo pathway. A dramatic increase in glycerol biosynthesis occurs due to inactivation of PFOR by ROS/RNS during extensive oxidative stress. Thus, conversion from pyruvate into acetyl-CoA is halted and sends a feedback to stop pyruvate production and activates the machinery towards glycerol biosynthesis. ROS/RNS (O_2, H_2O_2, O_2^-, NO·) are neutralized in coordination of several proteins like EhPFOR, Eh29/EhPrx, EhFDP, G protein, Ehmeth, EhNAOD, EhSIAF, EhPTPA, EhTrxR, EhSOD, EhADHE, EhHSP70, EhRbr, EhCP5, and peptidylprolyl isomerase to

maintain the intracellular redox state. In glycolysis, a pool of NADH and electrons are generated from reduced Fd, which can be subjected to transhydrogenation by NADP-dependent oxidoreductase or transhydrogenase to produce NADPH and may serve as the reductive equivalent donor to reduce O_2 and ROS by the antioxidant machinery. Divalent O_2 is converted to H_2O_2 with the help of Eh34, EhTrxR, and EhNO. Later on, H_2O_2 produces H_2O by EhPrx which is reduced by Eh34 or Trx. Fd can act as an alternative source of electron to facilitate the reduction of O_2 to H_2O without ROS generation via FDP system. FDP enzyme system can also detoxify the NO·generated by the parasite or from host immune response. Reduced Trx is converted to its oxidized form by TrxR through NADPH oxidation. EhSOD works to clean the harmful intracellular O_2^- by ORP. EhRbr with association of NROR protect mitosomes by converting H_2O_2 into H_2O. ISF and HCP have potential antioxidant capacity. *E. histolytica* can also decrease the redox potential of extracellular environment through the trans-PMET.

References

1. Ackers JCG, Diamond L, Duchene M, Cantellano M et al (1997) WHO/PAHO/UNESCO report. A consultation with experts on amoebiasis. Mexico City, Mexico 28-29 January, 1997. Epidemiol Bull 18(1):13–14
2. Haque R, Huston CD, Hughes M, Houpt E, Petri WA Jr (2003) Amebiasis. N Engl J Med 348(16):1565–1573. https://doi.org/10.1056/NEJMra022710
3. Stanley SL Jr (2003) Amoebiasis. Lancet 361(9362):1025–1034. https://doi.org/10.1016/S0140-6736(03)12830-9
4. Marie C, Petri WA Jr (2013) Amoebic dysentery. BMJ clinical evidence 2013, pii: 0918:1–16
5. Marie C, Petri WA Jr (2014) Regulation of virulence of *Entamoeba histolytica*. Annu Rev Microbiol 68:493–520. https://doi.org/10.1146/annurev-micro-091313-103550
6. Jarnagin WR (2012) Blumgart's surgery of the liver. Pancreas, Biliary Tract and
7. Paiva CN, Bozza MT (2014) Are reactive oxygen species always detrimental to pathogens? Antioxid Redox Signal 20(6):1000–1037. https://doi.org/10.1089/ars.2013.5447
8. Nagaraja S, Ankri S (2018) Utilization of different omic approaches to unravel stress response mechanisms in the parasite *Entamoeba histolytica*. Front Cell Infect Microbiol 8:19. https://doi.org/10.3389/fcimb.2018.00019
9. Mortimer L, Chadee K (2010) The immunopathogenesis of *Entamoeba histolytica*, vol 126. Exp Parasitol, vol 3, 2010/03/23 edn. doi:https://doi.org/10.1016/j.exppara.2010.03.005
10. Anderson P, Kedersha N (2002) Stressful initiations. J Cell Sci 115(Pt 16):3227–3234
11. Weber C, Guigon G, Bouchier C, Frangeul L, Moreira S, Sismeiro O, Gouyette C, Mirelman D, Coppee JY, Guillen N (2006) Stress by heat shock induces massive down regulation of genes and allows differential allelic expression of the Gal/GalNAc lectin in *Entamoeba histolytica*. Eukaryot Cell 5(5):871–875. https://doi.org/10.1128/EC.5.5.871-875.2006
12. Lisby M, Rothstein R (2004) DNA damage checkpoint and repair centers. Curr Opin Cell Biol 16(3):328–334. https://doi.org/10.1016/j.ceb.2004.03.011
13. Lisby M, Rothstein R (2004) DNA repair: keeping it together. Curr Biol 14(23):R994–R996. https://doi.org/10.1016/j.cub.2004.11.020
14. Lettier G, Feng Q, de Mayolo AA, Erdeniz N, Reid RJ, Lisby M, Mortensen UH, Rothstein R (2006) The role of DNA double-strand breaks in spontaneous homologous recombination in *S. cerevisiae*. PLoS Genet 2(11):e194. https://doi.org/10.1371/journal.pgen.0020194
15. Weber C, Marchat LA, Guillen N, Lopez-Camarillo C (2009) Effects of DNA damage induced by UV irradiation on gene expression in the protozoan parasite *Entamoeba histolytica*. Mol Biochem Parasitol 164(2):165–169. https://doi.org/10.1016/j.molbiopara.2008.12.005
16. Bracha R, Mirelman D (1984) Virulence of *Entamoeba histolytica* trophozoites. Effects of bacteria, microaerobic conditions, and metronidazole. J Exp Med 160(2):353–368. https://doi.org/10.1084/jem.160.2.353

17. Shahi P, Trebicz-Geffen M, Nagaraja S, Alterzon-Baumel S, Hertz R, Methling K, Lalk M, Ankri S (2016) Proteomic identification of oxidized proteins in *Entamoeba histolytica* by resin-assisted capture: insights into the role of arginase in resistance to oxidative stress. PLoS Negl Trop Dis 10(1):e0004340. https://doi.org/10.1371/journal.pntd.0004340
18. Fahey RC, Newton GL, Arrick B, Overdank-Bogart T, Aley SB (1984) *Entamoeba histolytica*: a eukaryote without glutathione metabolism. Science 224(4644):70–72. https://doi.org/10.1126/science.6322306
19. Pineda E, Perdomo D (2017) *Entamoeba histolytica* under oxidative stress: what countermeasure mechanisms are in place? Cell 6(4). https://doi.org/10.3390/cells6040044
20. Leitsch D, Kolarich D, Wilson IB, Altmann F, Duchene M (2007) Nitroimidazole action in *Entamoeba histolytica*: a central role for thioredoxin reductase. PLoS Biol 5(8):e211. https://doi.org/10.1371/journal.pbio.0050211
21. Pye VE, Tingey AP, Robson RL, Moody PC (2004) The structure and mechanism of serine acetyltransferase from *Escherichia coli*. J Biol Chem 279(39):40729–40736. https://doi.org/10.1074/jbc.M403751200
22. Hussain S, Ali V, Jeelani G, Nozaki T (2009) Isoform-dependent feedback regulation of serine O-acetyltransferase isoenzymes involved in L-cysteine biosynthesis of *Entamoeba histolytica*. Mol Biochem Parasitol 163(1):39–47. https://doi.org/10.1016/j.molbiopara.2008.09.006
23. Hirayama A, Kami K, Sugimoto M, Sugawara M, Toki N, Onozuka H, Kinoshita T, Saito N, Ochiai A, Tomita M, Esumi H, Soga T (2009) Quantitative metabolome profiling of colon and stomach cancer microenvironment by capillary electrophoresis time-of-flight mass spectrometry. Cancer Res 69(11):4918–4925. https://doi.org/10.1158/0008-5472.CAN-08-4806
24. Kellett GL, Brot-Laroche E, Mace OJ, Leturque A (2008) Sugar absorption in the intestine: the role of GLUT2. Annu Rev Nutr 28:35–54. https://doi.org/10.1146/annurev.nutr.28.061807.155518
25. Cummings JH, Macfarlane GT (1997) Role of intestinal bacteria in nutrient metabolism. JPEN J Parenter Enteral Nutr 21(6):357–365. https://doi.org/10.1177/0148607197021006357
26. Baumel-Alterzon S, Weber C, Guillen N, Ankri S (2013) Identification of dihydropyrimidine dehydrogenase as a virulence factor essential for the survival of *Entamoeba histolytica* in glucose-poor environments. Cell Microbiol 15(1):130–144. https://doi.org/10.1111/cmi.12036
27. Tovy A, Hertz R, Siman-Tov R, Syan S, Faust D, Guillen N, Ankri S (2011) Glucose starvation boosts *Entamoeba histolytica* virulence. PLoS Negl Trop Dis 5(8):e1247. https://doi.org/10.1371/journal.pntd.0001247
28. Beaulande M, Tarbouriech N, Hartlein M (1998) Human cytosolic asparaginyl-tRNA synthetase: cDNA sequence, functional expression in *Escherichia coli* and characterization as human autoantigen. Nucleic Acids Res 26(2):521–524. https://doi.org/10.1093/nar/26.2.521
29. Girjes AA, Hobson K, Chen P, Lavin MF (1995) Cloning and characterization of cDNA encoding a human arginyl-tRNA synthetase. Gene 164(2):347–350. https://doi.org/10.1016/0378-1119(95)00502-W
30. Thibeaux R, Weber C, Hon CC, Dillies MA, Ave P, Coppee JY, Labruyere E, Guillen N (2013) Identification of the virulence landscape essential for *Entamoeba histolytica* invasion of the human colon. PLoS Pathog 9(12):e1003824. https://doi.org/10.1371/journal.ppat.1003824
31. Park SJ, Lee SM, Lee J, Yong TS (2001) Differential gene expression by iron-limitation in *Entamoeba histolytica*. Mol Biochem Parasitol 114(2):257–260. https://doi.org/10.1016/S0166-6851(01)00264-X
32. Wandersman C, Delepelaire P (2004) Bacterial iron sources: from siderophores to hemophores. Annu Rev Microbiol 58:611–647. https://doi.org/10.1146/annurev.micro.58.030603.123811
33. Maralikova B, Ali V, Nakada-Tsukui K, Nozaki T, van der Giezen M, Henze K, Tovar J (2010) Bacterial-type oxygen detoxification and iron-sulfur cluster assembly in amoebal relict mitochondria. Cell Microbiol 12(3):331–342. https://doi.org/10.1111/j.1462-5822.2009.01397.x

34. Ali V, Shigeta Y, Tokumoto U, Takahashi Y, Nozaki T (2004) An intestinal parasitic protist, *Entamoeba histolytica*, possesses a non-redundant nitrogen fixation-like system for iron-sulfur cluster assembly under anaerobic conditions. J Biol Chem 279(16):16863–16874. https://doi.org/10.1074/jbc.M313314200
35. Tannich E, Bruchhaus I, Walter RD, Horstmann RD (1991) Pathogenic and non-pathogenic *Entamoeba histolytica*: identification and molecular cloning of an iron-containing superoxide dismutase. Mol Biochem Parasitol 49(1):61–71. https://doi.org/10.1016/0166-6851(91)90130-X
36. Espinosa A, Perdrizet G, Paz YMCG, Lanfranchi R, Phay M (2009) Effects of iron depletion on *Entamoeba histolytica* alcohol dehydrogenase 2 (EhADH2) and trophozoite growth: implications for antiamoebic therapy. J Antimicrob Chemother 63(4):675–678. https://doi.org/10.1093/jac/dkp015
37. Lee J, Park SJ, Yong TS (2008) Effect of iron on adherence and cytotoxicity of *Entamoeba histolytica* to CHO cell monolayers. Korean J Parasitol 46(1):37–40. https://doi.org/10.3347/kjp.2008.46.1.37
38. Hernandez-Cuevas NA, Weber C, Hon CC, Guillen N (2014) Gene expression profiling in *Entamoeba histolytica* identifies key components in iron uptake and metabolism. PLoS One 9(9):e107102. https://doi.org/10.1371/journal.pone.0107102
39. Biller L, Davis PH, Tillack M, Matthiesen J, Lotter H, Stanley SL Jr, Tannich E, Bruchhaus I (2010) Differences in the transcriptome signatures of two genetically related *Entamoeba histolytica* cell lines derived from the same isolate with different pathogenic properties. BMC Genomics 11:63. https://doi.org/10.1186/1471-2164-11-63
40. Jeelani G, Husain A, Sato D, Ali V, Suematsu M, Soga T, Nozaki T (2010) Two atypical L-cysteine-regulated NADPH-dependent oxidoreductases involved in redox maintenance, L-cystine and iron reduction, and metronidazole activation in the enteric protozoan *Entamoeba histolytica*. J Biol Chem 285(35):26889–26899. https://doi.org/10.1074/jbc.M110.106310
41. Perez-Victoria JM, Parodi-Talice A, Torres C, Gamarro F, Castanys S (2001) ABC transporters in the protozoan parasite *Leishmania*. Int microbiol 4(3):159–166. https://doi.org/10.1007/s10123-001-0031-2
42. Halliwell B, Gutteridge JMC (2015) Free radicals in biology and medicine, 5th edn. Oxford University Press, Oxford. https://doi.org/10.1093/acprof:oso/9780198717478.001.0001
43. Akbar MA, Chatterjee NS, Sen P, Debnath A, Pal A, Bera T, Das P (2004) Genes induced by a high-oxygen environment in *Entamoeba histolytica*. Mol Biochem Parasitol 133(2):187–196. https://doi.org/10.1016/j.molbiopara.2003.10.006
44. Vicente JB, Ehrenkaufer GM, Saraiva LM, Teixeira M, Singh U (2009) *Entamoeba histolytica* modulates a complex repertoire of novel genes in response to oxidative and nitrosative stresses: implications for amebic pathogenesis. Cell Microbiol 11(1):51–69. https://doi.org/10.1111/j.1462-5822.2008.01236.x
45. Santi-Rocca J, Smith S, Weber C, Pineda E, Hon CC, Saavedra E, Olivos-Garcia A, Rousseau S, Dillies MA, Coppee JY, Guillen N (2012) Endoplasmic reticulum stress-sensing mechanism is activated in *Entamoeba histolytica* upon treatment with nitric oxide. PLoS One 7(2):e31777. https://doi.org/10.1371/journal.pone.0031777
46. Andersson JO, Hirt RP, Foster PG, Roger AJ (2006) Evolution of four gene families with patchy phylogenetic distributions: influx of genes into protist genomes. BMC Evol Biol 6:27. https://doi.org/10.1186/1471-2148-6-27
47. Andersson JO, Sjogren AM, Davis LA, Embley TM, Roger AJ (2003) Phylogenetic analyses of diplomonad genes reveal frequent lateral gene transfers affecting eukaryotes. Curr Biol 13(2):94–104. https://doi.org/10.1016/S0960-9822(03)00003-4
48. Pineda E, Encalada R, Rodriguez-Zavala JS, Olivos-Garcia A, Moreno-Sanchez R, Saavedra E (2010) Pyruvate:ferredoxin oxidoreductase and bifunctional aldehyde-alcohol dehydrogenase are essential for energy metabolism under oxidative stress in *Entamoeba histolytica*. FEBS J 277(16):3382–3395. https://doi.org/10.1111/j.1742-4658.2010.07743.x

49. Reeves RE (1984) Metabolism of *Entamoeba histolytica* Schaudinn, 1903. Adv Parasitol 23:105–142
50. Montalvo FE, Reeves RE, Warren LG (1971) Aerobic and anaerobic metabolism in *Entamoeba histolytica*. Exp Parasitol 30(2):249–256. https://doi.org/10.1016/0014-4894(71)90089-0
51. Reeves RE, Warren LG, Susskind B, Lo HS (1977) An energy-conserving pyruvate-to-acetate pathway in *Entamoeba histolytica*. Pyruvate synthase and a new acetate thiokinase. J Biol Chem 252(2):726–731
52. Lo HS, Reeves RE (1978) Pyruvate-to-ethanol pathway in *Entamoeba histolytica*. Biochem J 171(1):225–230. https://doi.org/10.1042/bj1710225
53. Townson SM, Upcroft JA, Upcroft P (1996) Characterisation and purification of pyruvate:ferredoxin oxidoreductase from *Giardia duodenalis*. Mol Biochem Parasitol 79(2):183–193. https://doi.org/10.1016/0166-6851(96)02661-8
54. Williams K, Lowe PN, Leadlay PF (1987) Purification and characterization of pyruvate: ferredoxin oxidoreductase from the anaerobic protozoon *Trichomonas vaginalis*. Biochem J 246(2):529–536. https://doi.org/10.1042/bj2460529
55. Bruchhaus I, Tannich E (1993) Analysis of the genomic sequence encoding the 29-kDa cysteine-rich protein of *Entamoeba histolytica*. Trop Med Parasitol 44(2):116–118
56. Flores BM, Batzer MA, Stein MA, Petersen C, Diedrich DL, Torian BE (1993) Structural analysis and demonstration of the 29 kDa antigen of pathogenic *Entamoeba histolytica* as the major accessible free thiol-containing surface protein. Mol Microbiol 7(5):755–763. https://doi.org/10.1111/j.1365-2958.1993.tb01166.x
57. Bruchhaus I, Richter S, Tannich E (1997) Removal of hydrogen peroxide by the 29 kDa protein of *Entamoeba histolytica*. Biochem J 326(Pt 3):785–789. https://doi.org/10.1042/bj3260785
58. Sen A, Chatterjee NS, Akbar MA, Nandi N, Das P (2007) The 29-kilodalton thiol-dependent peroxidase of *Entamoeba histolytica* is a factor involved in pathogenesis and survival of the parasite during oxidative stress. Eukaryot Cell 6(4):664–673. https://doi.org/10.1128/EC.00308-06
59. Cheng XJ, Yoshihara E, Takeuchi T, Tachibana H (2004) Molecular characterization of peroxiredoxin from *Entamoeba moshkovskii* and a comparison with *Entamoeba histolytica*. Mol Biochem Parasitol 138(2):195–203. https://doi.org/10.1016/j.molbiopara.2004.08.009
60. Hughes MA, Lee CW, Holm CF, Ghosh S, Mills A, Lockhart LA, Reed SL, Mann BJ (2003) Identification of *Entamoeba histolytica* thiol-specific antioxidant as a GalNAc lectin-associated protein. Mol Biochem Parasitol 127(2):113–120. https://doi.org/10.1016/S0166-6851(02)00326-2
61. Jeelani G, Nozaki T (2016) *Entamoeba* thiol-based redox metabolism: A potential target for drug development. Mol Biochem Parasitol 206(1–2):39–45. https://doi.org/10.1016/j.molbiopara.2016.01.004
62. Kurtz DM (2007) Flavo-diiron enzymes: nitric oxide or dioxygen reductases? Dalton T 37:4115–4121. https://doi.org/10.1039/b710047g
63. Vicente JB, Justino MC, Goncalves VL, Saraiva LM, Teixeira M (2008) Biochemical, spectroscopic, and thermodynamic properties of flavodiiron proteins. Methods Enzymol 437:21–45. https://doi.org/10.1016/S0076-6879(07)37002-X
64. Saraiva LM, Vicente JB, Teixeira M (2004) The role of the flavodiiron proteins in microbial nitric oxide detoxification. Adv Microb Physiol 49:77–129. https://doi.org/10.1016/S0065-2911(04)49002-X
65. Loftus B, Anderson I, Davies R, Alsmark UC, Samuelson J, Amedeo P, Roncaglia P, Berriman M, Hirt RP, Mann BJ, Nozaki T, Suh B, Pop M, Duchene M, Ackers J, Tannich E, Leippe M, Hofer M, Bruchhaus I, Willhoeft U, Bhattacharya A, Chillingworth T, Churcher C, Hance Z, Harris B, Harris D, Jagels K, Moule S, Mungall K, Ormond D, Squares R, Whitehead S, Quail MA, Rabbinowitsch E, Norbertczak H, Price C, Wang Z, Guillen N, Gilchrist C, Stroup SE, Bhattacharya S, Lohia A, Foster PG, Sicheritz-Ponten T, Weber C, Singh U, Mukherjee C, El-Sayed NM, Petri WA Jr, Clark CG, Embley TM, Barrell B, Fraser CM, Hall N (2005)

The genome of the protist parasite *Entamoeba histolytica*. Nature 433(7028):865–868. https://doi.org/10.1038/nature03291
66. Di Matteo A, Scandurra FM, Testa F, Forte E, Sarti P, Brunori M, Giuffre A (2008) The O2-scavenging flavodiiron protein in the human parasite *Giardia intestinalis*. J Biol Chem 283(7):4061–4068. https://doi.org/10.1074/jbc.M705605200
67. Smutna T, Goncalves VL, Saraiva LM, Tachezy J, Teixeira M, Hrdy I (2009) Flavodiiron protein from *Trichomonas vaginalis* hydrogenosomes: the terminal oxygen reductase. Eukaryot Cell 8(1):47–55. https://doi.org/10.1128/EC.00276-08
68. Mastronicola D, Giuffre A, Testa F, Mura A, Forte E, Bordi E, Pucillo LP, Fiori PL, Sarti P (2011) *Giardia intestinalis* escapes oxidative stress by colonizing the small intestine: A molecular hypothesis. IUBMB Life 63(1):21–25. https://doi.org/10.1002/iub.409
69. Cai CQ, Guo H, Schroeder RA, Punzalan C, Kuo PC (2000) Nitric oxide-dependent ribosomal RNA cleavage is associated with inhibition of ribosomal peptidyl transferase activity in ANA-1 murine macrophages. J Immunol 165(7):3978–3984. https://doi.org/10.4049/jimmunol.165.7.3978
70. Kim YM, Son K, Hong SJ, Green A, Chen JJ, Tzeng E, Hierholzer C, Billiar TR (1998) Inhibition of protein synthesis by nitric oxide correlates with cytostatic activity: nitric oxide induces phosphorylation of initiation factor eIF-2 alpha. Mol Med 4(3):179–190
71. Hertz R, Tovy A, Kirschenbaum M, Geffen M, Nozaki T, Adir N, Ankri S (2014) The *Entamoeba histolytica* Dnmt2 homolog (Ehmeth) confers resistance to nitrosative stress. Eukaryot Cell 13(4):494–503. https://doi.org/10.1128/EC.00031-14
72. Illi B, Colussi C, Grasselli A, Farsetti A, Capogrossi MC, Gaetano C (2009) NO sparks off chromatin: tales of a multifaceted epigenetic regulator. Pharmacol Ther 123(3):344–352. https://doi.org/10.1016/j.pharmthera.2009.05.003
73. Tovy A, Siman Tov R, Gaentzsch R, Helm M, Ankri S (2010) A new nuclear function of the *Entamoeba histolytica* glycolytic enzyme enolase: the metabolic regulation of cytosine-5 methyltransferase 2 (Dnmt2) activity. PLoS Pathog 6(2):e1000775. https://doi.org/10.1371/journal.ppat.1000775
74. Vogel C, Silva GM, Marcotte EM (2011) Protein expression regulation under oxidative stress. Mol Cell Proteomics: MCP 10(12):M111009217. https://doi.org/10.1074/mcp.M111.009217
75. Shahi P, Trebicz-Geffen M, Nagaraja S, Hertz R, Alterzon-Baumel S, Methling K, Lalk M, Mazumder M, Samudrala G, Ankri S (2016) N-acetyl ornithine deacetylase is a moonlighting protein and is involved in the adaptation of Entamoeba histolytica to nitrosative stress. Sci Rep 6:36323. https://doi.org/10.1038/srep36323
76. Aguilar-Rojas A, Olivo-Marin JC, Guillen N (2016) The motility of *Entamoeba histolytica*: finding ways to understand intestinal amoebiasis. Curr Opin Microbiol 34:24–30. https://doi.org/10.1016/j.mib.2016.07.016
77. Rastew E, Vicente JB, Singh U (2012) Oxidative stress resistance genes contribute to the pathogenic potential of the anaerobic protozoan parasite, *Entamoeba histolytica*. Int J Parasitol 42(11):1007–1015. https://doi.org/10.1016/j.ijpara.2012.08.006
78. Elnekave K, Siman-Tov R, Ankri S (2003) Consumption of L-arginine mediated by *Entamoeba histolytica* L-arginase (EhArg) inhibits amoebicidal activity and nitric oxide production by activated macrophages. Parasite Immunol 25(11–12):597–608. https://doi.org/10.1111/j.0141-9838.2004.00669.x
79. Burgess SL, Petri WA Jr (2016) The intestinal bacterial microbiome and *E. histolytica* infection. Curr Trop Med Rep 3:71–74. https://doi.org/10.1007/s40475-016-0083-1
80. Mirelman D, Feingold C, Wexler A, Bracha R (1983) Interactions between *Entamoeba histolytica*, bacteria and intestinal cells. Ciba Found Symp 99:2–30
81. Paniagua GL, Monroy E, Garcia-Gonzalez O, Alonso J, Negrete E, Vaca S (2007) Two or more enteropathogens are associated with diarrhoea in Mexican children. Ann Clin Microbiol Antimicrob 6:17. https://doi.org/10.1186/1476-0711-6-17
82. Gilchrist CA, Petri SE, Schneider BN, Reichman DJ, Jiang N, Begum S, Watanabe K, Jansen CS, Elliott KP, Burgess SL, Ma JZ, Alam M, Kabir M, Haque R, Petri WA Jr (2016) Role

of the gut microbiota of children in diarrhea due to the protozoan *Parasite Entamoeba histolytica*. J Infect Dis 213(10):1579–1585. https://doi.org/10.1093/infdis/jiv772
83. Varet H, Shaulov Y, Sismeiro O, Trebicz-Geffen M, Legendre R, Coppee JY, Ankri S, Guillen N (2018) Enteric bacteria boost defences against oxidative stress in *Entamoeba histolytica*. Sci Rep 8(1):9042. https://doi.org/10.1038/s41598-018-27086-w
84. Arhets P, Gounon P, Sansonetti P, Guillen N (1995) Myosin II is involved in capping and uroid formation in the human pathogen *Entamoeba histolytica*. Infect Immun 63(11):4358–4367
85. Coudrier E, Amblard F, Zimmer C, Roux P, Olivo-Marin JC, Rigothier MC, Guillen N (2005) Myosin II and the Gal-GalNAc lectin play a crucial role in tissue invasion by *Entamoeba histolytica*. Cell Microbiol 7(1):19–27. https://doi.org/10.1111/j.1462-5822.2004.00426.x
86. Perdomo D, Manich M, Syan S, Olivo-Marin JC, Dufour AC, Guillen N (2016) Intracellular traffic of the lysine and glutamic acid rich protein KERP1 reveals features of endomembrane organization in *Entamoeba histolytica*. Cell Microbiol 18(8):1134–1152. https://doi.org/10.1111/cmi.12576
87. Kumar N, Somlata MM, Dutta P, Maiti S, Gourinath S (2014) EhCoactosin stabilizes actin filaments in the protist parasite *Entamoeba histolytica*. PLoS Pathog 10(9):e1004362. https://doi.org/10.1371/journal.ppat.1004362
88. Hertz R, Ben Lulu S, Shahi P, Trebicz-Geffen M, Benhar M, Ankri S (2014) Proteomic identification of S-nitrosylated proteins in the parasite *Entamoeba histolytica* by resin-assisted capture: insights into the regulation of the Gal/GalNAc lectin by nitric oxide. PLoS One 9(3):e91518. https://doi.org/10.1371/journal.pone.0091518
89. Imlay JA (2003) Pathways of oxidative damage. Annu Rev Microbiol 57:395–418. https://doi.org/10.1146/annurev.micro.57.030502.090938
90. Apel K, Hirt H (2004) Reactive oxygen species: metabolism, oxidative stress, and signal transduction. Annu Rev Plant Biol 55:373–399. https://doi.org/10.1146/annurev.arplant.55.031903.141701
91. Perrone GG, Tan SX, Dawes IW (2008) Reactive oxygen species and yeast apoptosis. Biochim Biophys Acta 1783(7):1354–1368. https://doi.org/10.1016/j.bbamcr.2008.01.023
92. Clement MV, Pervaiz S (1999) Reactive oxygen intermediates regulate cellular response to apoptotic stimuli: an hypothesis. Free Radic Res 30(4):247–252. https://doi.org/10.1080/10715769900300271
93. Nandi N, Sen A, Banerjee R, Kumar S, Kumar V, Ghosh AN, Das P (2010) Hydrogen peroxide induces apoptosis-like death in *Entamoeba histolytica* trophozoites. Microbiology 156(Pt 7):1926–1941. https://doi.org/10.1099/mic.0.034066-0
94. Ghosh AS, Dutta S, Raha S (2010) Hydrogen peroxide-induced apoptosis-like cell death in *Entamoeba histolytica*. Parasitol Int 59(2):166–172. https://doi.org/10.1016/j.parint.2010.01.001
95. Temple MD, Perrone GG, Dawes IW (2005) Complex cellular responses to reactive oxygen species. Trends Cell Biol 15(6):319–326. https://doi.org/10.1016/j.tcb.2005.04.003
96. Ralser M, Wamelink MM, Kowald A, Gerisch B, Heeren G, Struys EA, Klipp E, Jakobs C, Breitenbach M, Lehrach H, Krobitsch S (2007) Dynamic rerouting of the carbohydrate flux is key to counteracting oxidative stress. J Biol 6(4):10. https://doi.org/10.1186/jbiol61
97. Bogdan C, Rollinghoff M, Diefenbach A (2000) Reactive oxygen and reactive nitrogen intermediates in innate and specific immunity. Curr Opin Immunol 12(1):64–76. https://doi.org/10.1016/S0952-7915(99)00052-7
98. Mehlotra RK (1996) Antioxidant defense mechanisms in parasitic protozoa. Crit Rev Microbiol 22(4):295–314. https://doi.org/10.3109/10408419609105484
99. Jackson JB (1991) The proton-translocating nicotinamide adenine dinucleotide transhydrogenase. J Bioenerg Biomembr 23(5):715–741. https://doi.org/10.1007/BF00785998
100. Yousuf MA, Mi-ichi F, Nakada-Tsukui K, Nozaki T (2010) Localization and targeting of an unusual pyridine nucleotide transhydrogenase in *Entamoeba histolytica*. Eukaryot Cell 9(6):926–933. https://doi.org/10.1128/EC.00011-10

101. Husain A, Sato D, Jeelani G, Soga T, Nozaki T (2012) Dramatic increase in glycerol biosynthesis upon oxidative stress in the anaerobic protozoan parasite *Entamoeba histolytica*. PLoS Negl Trop Dis 6(9):e1831. https://doi.org/10.1371/journal.pntd.0001831
102. Ramos-Martinez E, Olivos-Garcia A, Saavedra E, Nequiz M, Sanchez EC, Tello E, El-Hafidi M, Saralegui A, Pineda E, Delgado J, Montfort I, Perez-Tamayo R (2009) *Entamoeba histolytica*: oxygen resistance and virulence. Int J Parasitol 39(6):693–702. https://doi.org/10.1016/j.ijpara.2008.11.004
103. Ramos E, Olivos-Garcia A, Nequiz M, Saavedra E, Tello E, Saralegui A, Montfort I, Perez Tamayo R (2007) *Entamoeba histolytica*: apoptosis induced in vitro by nitric oxide species. Exp Parasitol 116(3):257–265. https://doi.org/10.1016/j.exppara.2007.01.011
104. Susskind BM, Warren LG, Reeves RE (1982) A pathway for the interconversion of hexose and pentose in the parasitic amoeba *Entamoeba histolytica*. Biochem J 204(1):191–196
105. Pollak N, Dolle C, Ziegler M (2007) The power to reduce: pyridine nucleotides--small molecules with a multitude of functions. Biochem J 402(2):205–218. https://doi.org/10.1042/BJ20061638
106. Chavez-Munguia B, Martinez-Palomo A (2011) High-resolution electron microscopical study of cyst walls of *Entamoeba* spp. J Eukaryot Microbiol 58(6):480–486. https://doi.org/10.1111/j.1550-7408.2011.00576.x
107. Arroyo-Begovich A, Carabez-Trejo A, Ruiz-Herrera J (1978) Composition of the cell wall of *Entamoeba invadens* cysts. Arch Invest Med (Mex), 9(Suppl 1). 1978/01/01 edn. https://doi.org/10.2307/3280662
108. Aguilar-Diaz H, Diaz-Gallardo M, Laclette JP, Carrero JC (2010) In vitro induction of *Entamoeba histolytica* cyst-like structures from trophozoites. PLoS Negl Trop Dis 4(2):e607. https://doi.org/10.1371/journal.pntd.0000607
109. Anderson IJ, Loftus BJ (2005) *Entamoeba histolytica*: observations on metabolism based on the genome sequence. Exp Parasitol 110(3):173–177. https://doi.org/10.1016/j.exppara.2005.03.010
110. Husain A, Sato D, Jeelani G, Mi-ichi F, Ali V, Suematsu M, Soga T, Nozaki T (2010) Metabolome analysis revealed increase in S-methylcysteine and phosphatidylisopropanolamine synthesis upon L-cysteine deprivation in the anaerobic protozoan parasite *Entamoeba histolytica*. J Biol Chem 285(50):39160–39170. https://doi.org/10.1074/jbc.M110.167304
111. Nozaki T, Ali V, Tokoro M (2005) Sulfur-containing amino acid metabolism in parasitic protozoa. Adv Parasitol 60:1–99. https://doi.org/10.1016/S0065-308X(05)60001-2
112. Ali V, Nozaki T (2007) Current therapeutics, their problems, and sulfur-containing-amino-acid metabolism as a novel target against infections by "amitochondriate" protozoan parasites. Clin Microbiol Rev 20(1):164–187. https://doi.org/10.1128/CMR.00019-06
113. Tokoro M, Asai T, Kobayashi S, Takeuchi T, Nozaki T (2003) Identification and characterization of two isoenzymes of methionine gamma-lyase from *Entamoeba histolytica*: a key enzyme of sulfur-amino acid degradation in an anaerobic parasitic protist that lacks forward and reverse trans-sulfuration pathways. J Biol Chem 278(43):42717–42727. https://doi.org/10.1074/jbc.M212414200
114. Husain A, Jeelani G, Sato D, Nozaki T (2011) Global analysis of gene expression in response to L-Cysteine deprivation in the anaerobic protozoan parasite *Entamoeba histolytica*. BMC Genomics 12:275. https://doi.org/10.1186/1471-2164-12-275
115. Colussi C, Albertini MC, Coppola S, Rovidati S, Galli F, Ghibelli L (2000) H2O2-induced block of glycolysis as an active ADP-ribosylation reaction protecting cells from apoptosis. FASEB J 14(14):2266–2276. https://doi.org/10.1096/fj.00-0074com
116. Shenton D, Grant CM (2003) Protein S-thiolation targets glycolysis and protein synthesis in response to oxidative stress in the yeast *Saccharomyces cerevisiae*. Biochem J 374(Pt 2):513–519. https://doi.org/10.1042/BJ20030414
117. Lian LY, Al-Helal M, Roslaini AM, Fisher N, Bray PG, Ward SA, Biagini GA (2009) Glycerol: an unexpected major metabolite of energy metabolism by the human malaria parasite. Malar J 8:38. https://doi.org/10.1186/1475-2875-8-38

118. Hammond DJ, Bowman IB (1980) Studies on glycerol kinase and its role in ATP synthesis in *Trypanosoma brucei*. Mol Biochem Parasitol 2(2):77–91. https://doi.org/10.1016/0166-6851(80)90033-X
119. Chapman A, Linstead DJ, Lloyd D, Williams J (1985) 13C-NMR reveals glycerol as an unexpected major metabolite of the protozoan parasite *Trichomonas vaginalis*. FEBS Lett 191(2):287–292. https://doi.org/10.1016/0014-5793(85)80026-0
120. Mar-Aguilar F, Trevino V, Salinas-Hernandez JE, Tamez-Guerrero MM, Barron-Gonzalez MP, Morales-Rubio E, Trevino-Neavez J, Verduzco-Martinez JA, Morales-Vallarta MR, Resendez-Perez D (2013) Identification and characterization of microRNAs from *Entamoeba histolytica* HM1-IMSS. PLoS One 8(7):e68202. https://doi.org/10.1371/journal.pone.0068202
121. Morf L, Pearson RJ, Wang AS, Singh U (2013) Robust gene silencing mediated by antisense small RNAs in the pathogenic protist *Entamoeba histolytica*. Nucleic Acids Res 41(20):9424–9437. https://doi.org/10.1093/nar/gkt717
122. Zhang H, Alramini H, Tran V, Singh U (2011) Nucleus-localized antisense small RNAs with 5′-polyphosphate termini regulate long term transcriptional gene silencing in *Entamoeba histolytica* G3 strain. J Biol Chem 286(52):44467–44479. https://doi.org/10.1074/jbc.M111.278184
123. Zhang H, Ehrenkaufer GM, Pompey JM, Hackney JA, Singh U (2008) Small RNAs with 5′-polyphosphate termini associate with a Piwi-related protein and regulate gene expression in the single-celled eukaryote *Entamoeba histolytica*. PLoS Pathog 4(11):e1000219. https://doi.org/10.1371/journal.ppat.1000219
124. Geisler S, Coller J (2013) RNA in unexpected places: long non-coding RNA functions in diverse cellular contexts. Nat Rev Mol Cell Biol 14(11):699–712. https://doi.org/10.1038/nrm3679
125. Rinn JL, Chang HY (2012) Genome regulation by long noncoding RNAs. Annu Rev Biochem 81:145–166. https://doi.org/10.1146/annurev-biochem-051410-092902
126. Shrimal S, Bhattacharya S, Bhattacharya A (2010) Serum-dependent selective expression of EhTMKB1-9, a member of *Entamoeba histolytica* B1 family of transmembrane kinases. PLoS Pathog 6(6):e1000929. https://doi.org/10.1371/journal.ppat.1000929
127. Saha A, Bhattacharya S, Bhattacharya A (2016) Serum stress responsive gene EhslncRNA of *Entamoeba histolytica* is a novel long noncoding RNA. Sci Rep 6:27476. https://doi.org/10.1038/srep27476
128. Ray AK, Naiyer S, Singh SS, Bhattacharya A, Bhattacharya S (2018) Application of SHAPE reveals in vivo RNA folding under normal and growth-stressed conditions in the human parasite *Entamoeba histolytica*. Mol Biochem Parasitol 219:42–51. https://doi.org/10.1016/j.molbiopara.2017.11.003
129. Shahi P, Trebicz-Geffen M, Nagaraja S, Hertz R, Baumel-Alterzon S, Methling K, Lalk M, Mazumder M, Samudrala G, Ankri S (2016) N-acetyl ornithine deacetylase is a moonlighting protein and is involved in the adaptation of *Entamoeba histolytica* to nitrosative stress. Sci Rep 6:36323. https://doi.org/10.1038/srep36323
130. Satish S, Bakre AA, Bhattacharya S, Bhattacharya A (2003) Stress-dependent expression of a polymorphic, charged antigen in the protozoan parasite *Entamoeba histolytica*. Infect Immun 71(8):4472–4486. https://doi.org/10.1128/IAI.71.8.4472-4486.2003
131. Vicente JB, Tran V, Pinto L, Teixeira M, Singh U (2012) A detoxifying oxygen reductase in the anaerobic protozoan *Entamoeba histolytica*. Eukaryot Cell 11(9):1112–1118. https://doi.org/10.1128/EC.00149-12
132. Arias DG, Regner EL, Iglesias AA, Guerrero SA (2012) *Entamoeba histolytica* thioredoxin reductase: molecular and functional characterization of its atypical properties. Biochim Biophys Acta 1820(12):1859–1866. https://doi.org/10.1016/j.bbagen.2012.08.020
133. Pearson RJ, Morf L, Singh U (2013) Regulation of H2O2 stress-responsive genes through a novel transcription factor in the protozoan pathogen *Entamoeba histolytica*. J Biol Chem 288(6):4462–4474. https://doi.org/10.1074/jbc.M112.423467

134. Santos F, Nequiz M, Hernandez-Cuevas NA, Hernandez K, Pineda E, Encalada R, Guillen N, Luis-Garcia E, Saralegui A, Saavedra E, Perez-Tamayo R, Olivos-Garcia A (2015) Maintenance of intracellular hypoxia and adequate heat shock response are essential requirements for pathogenicity and virulence of *Entamoeba histolytica*. Cell Microbiol 17(7):1037–1051. https://doi.org/10.1111/cmi.12419
135. Manochitra K, Parija SC (2017) In-silico prediction and modeling of the *Entamoeba histolytica* proteins: Serine-rich *Entamoeba histolytica* protein and 29 kDa Cysteine-rich protease. PeerJ 5:e3160. https://doi.org/10.7717/peerj.3160
136. Mares RE, Ramos MA (2018) An amebic protein disulfide isomerase (PDI) complements the yeast PDI1 mutation but is unable to support cell viability under ER or thermal stress. FEBS open bio 8(1):49–55. https://doi.org/10.1002/2211-5463.12350

OPEN ACCESS
Haya: The Saudi Journal of Life Sciences
Abbreviated Key Title: Haya Saudi J Life Sci
ISSN 2415-623X (Print) |ISSN 2415-6221 (Online)
Scholars Middle East Publishers, Dubai, United Arab Emirates
Journal homepage: https://saudijournals.com/sjls

Original Research Article

In Silico Analysis of Molecular Interaction of EhSir2a with its Interacting Proteins from Human Pathogen *Entamoeba histolytica*

Pinaki Biswas[1], Somasri Dam[2*]

[1]Department of Microbiology, The University of Burdwan, Burdwan-713104, West Bengal, India
[2]Assistant Professor, Department of Microbiology, The University of Burdwan, Burdwan-713104, West Bengal, India

DOI: 10.36348/sjls.2020.v05i08.002 | **Received:** 30.07.2020 | **Accepted:** 07.08.2020 | **Published:** 22.08.2020

***Corresponding author:** Somasri Dam

Abstract

The human pathogen, *Entamoeba histolytica* contains four Sir2 homologs in its genome. We have designed the 3D tertiary structure of EhSir2a and its interacting partners by comparative homology modeling and studied their interaction by molecular docking. Sir2 proteins are known to interact with their substrates through the deacetylase domain present in its C-terminus. Interestingly, EhSir2a contains a unique Zn finger domain at its N terminus and this is not present in any known Sir2 protein. This study shows that EhSir2a may interact with this N-terminal residue also. It interacts with its substrate, elongation factor EhEF2 through this zinc-finger domain. The interaction sites are different for alpha-tubulin homologs, the other substrates of EhSir2a identified by yeast two-hybrid library screening. The coordinate files of the best-modeled structure for EhSir2a and its interacting proteins were processed for protein-protein docking using ClusPro v2.0 and HawkDock server. Tyr432, Asn422, Arg408 residues of α-tubulin are essential for interaction with EhSir2a. Here we report that molecular interactions of EhSir2a with its interacting partners are not restricted to the conserved NAD^+ dependent deacetylase domain; it may also involve the N-terminal residue.

Keywords: *Entamoeba histolytica*, Sirtuin, Homology modelling, Molecular docking, Gromacs.

INTRODUCTION

The protozoan parasite *Entamoeba histolytica* is an etiological agent of amoebiasis in humans. Amoebiasis was recorded as the third leading cause of death from parasitic infection worldwide, with its greatest impact on the people of developing countries [1]. Approximately 50 million people worldwide suffer from invasive amoebic infection each year, resulting in 40-100 thousand deaths annually [2, 3]. Unicellular protozoa like *E. histolytica* is the early evolutionary divergent of eukaryotic lineage. The mode of nutrition in many such protozoa is parasitic which makes them medically significant. Thus, *E. histolytica* being a protozoan parasite may serve as a model organism to study not only their cellular biology and evolution but also to understand the mechanism of pathogenesis and identification of potential drug targets. *E. histolytica* is different from other pathogenic protozoa by having an unusual mode of cell cycle events [4-8]. The parasite is prone to oxidative stress due to the lack of most of the antioxidant defense mechanisms such as glutathione peroxidase, glutathione reductase, and catalase enzymes [9, 10]. Identification of different essential proteins in *E. histolytica* may enlighten us with their physiological role and related interactome. Sirtuins are NAD^+-dependent class III histone deacetylases which are well conserved and widely distributed among all domains of life from archaea to eukarya [11]. Deacetylation of substrates like histone and other non-histone proteins require NAD^+ as a co-substrate and nicotinamide and O-acetyl-ADP-ribose are released as metabolites [12]. Increasing cellular concentration of nicotinamide may feedback-inhibit sirtuin activity by non-competitive binding [13, 14]. Likewise, the other metabolite, O-acetyl-ADP-ribose has also been reported as a signaling molecule [15-18]. Sirtuin may provide a direct link between metabolic programming and the control of gene expression. Previous study of sirtuins in protozoan parasites like, *Entamoeba histolytica* [19], *Plasmodium falciparum* [20, 21], *Leishmania donovani* [22, 23], *Leishmania infantum* [24-28], *Leishmania amazonensis* [29], *Eimeria tenella* [30], *Cryptosporidium parvum* [31], *Cryptosporidium hominis* [32], *Trypanosoma cruzi* [33, 34], *Trypanosoma brucei* [35] and *Giardia lambia* [36, 37] reflect their versatile functionality in cellular processes [38-40].

EhSir2a regulates microtubule assembly during cell cycle progression by tubulin deacetylation. The interactors of EhSir2a include two alpha-tubulin homologs (EhAT1, Acc. no. XP_650067.1 and EhAT2, Acc. no. XP_653419.1), elongation factor 2 (EhEF2, Acc. no. XP_651009.2), putative proteasome beta subunit (EhPBST3, Acc no. XP_655858.1), translation initiation factor (EhMIF4G, Acc. no. XP_654481.1), phospholipase B (EhPLB1, Acc. no. XP_654113.1) and serine/threonine phosphatase [19]. In the present study, we have constructed a three-dimensional structural model of EhSir2a and its interactors (EhAT1, EhAT2, EhEF2, and EhPBST3). The molecular interactions between these proteins have been reported here.

MATERIAL AND METHODS

EhSir2a interacting proteins

EhSir2a interacting proteins were searched using the FASTA sequence of EhSir2a as a query in the latest version of the STRING v11.0 database at a confidence level of 0.4. Interaction of EhSir2a with its protein partners was investigated based on text mining, co-expression, experimental data, known metabolic, and signal transduction pathways [41, 42].

Homology modeling and structural analysis

The amino acid sequence of EhSir2a (Acc. Id: XP_657434.1) and its interactors (EhAT1, Acc. Id: XP_650067.1; EhAT2, Acc. Id: XP_653419.1; EhEF2, Acc. Id: XP_651009.2; EhPBST3, Acc. Id: XP_655858.1) were retrieved from NCBI protein database in FASTA format. The interactors were obtained by yeast two-hybrid screening against the cDNA library and also by STRING analysis. For homology modeling, the SWISS-MODEL server is used to search a suitable template in SWISS-MODEL Template Library for evolutionary related structures matching the target sequence [43]. Among all the templates, the best one was determined by an optimal combination of high coverage, sequence similarity, sequence identity, and low resolution. Homology based modeling was done with MODELLER v9.20 [44], and Galaxy TBM followed by Galaxy Refine [45]. The quality and the integrity of the predicted models were evaluated by QMEAN scoring function [46], Ramachandran plot (RAMPAGE) [47], ResProx (Resolution-by-proxy) [48], ProQ (Protein quality prediction) [49], ProSA (Protein Structure Analysis) [50] and SAVES v5 (Verify 3D, ERRAT, PROVE, PROCHECK, WHATCHECK). All the protein structures were visually represented with the help of PyMOL. Protein structures were analyzed by the PDBsum tool [51].

Molecular docking of EhSir2a and its interactors

Molecular Docking study was performed by ClusPro (v2.0), a blind rigid PIPER docking program based on fast Fourier transformation to generate low energy interaction conformations of a protein-protein complex using the pairwise docking potentials. Stable interaction complex was refined by filtering and clustering of docked confrontation using pairwise RMSD subsequently stabilization using Monte–Carlo simulations. ClusPro presents the protein-protein interaction in four different modes: Balanced, Electrostatic-favoured, Hydrophobic-favored, and VdW+Elec favored. Protein-protein interactions with the highest members in cluster formation of each interaction mode were selected [52-54]. HawkDock Server treats a comparatively smaller protein as a flexible and larger protein as a stationary receptor. ATTRACT docking algorithm, HawkRank scoring function with MM/GBSA free energy decomposition analysis was employed to predict the binding free energy and decompose the free energy contributions to the binding free energy of a protein-protein complex in per residue. The best ten models of interacting proteins were re-ranked by MM/GBSA (Molecular Mechanics energies combined with the Generalized Born and Surface Area continuum solvation) calculation [55, 56]. All protein-protein interactions were represented diagrammatically using the LigPlot program [57]. All scoring functions and free energy were calculated as described in respective references.

Prediction of the functional and biological role of EhSir2a

COFACTOR server was used to predict the functional and biological significance of protein molecules by analyzing its structure, sequence, and protein-protein interaction. 3D structural model file EhSir2a in PDB format was submitted and threaded through the BioLiP protein function database on local and as well as global scale to identify functional sites and homologies. Functional insights, including Gene Ontology (GO), Enzyme Commission (EC), and ligand-binding sites are predicted from the best templates depending on functional homology. For GO, it acquires data by sequence, sequence-profile alignments from UniProt-GOA, and by protein-protein interaction from STRING [58, 59].

Molecular Dynamics Simulation

Molecular dynamics (MD) simulation of Ehsir2a was performed individually using GROMACS 5.1.4 [60]. The geometry of each complex was regularized using the GROMOS96 54a7 force field [61]. All the structures were placed in the center of a cubic box with a minimum distance of 1 nm between the protein and the wall of the box on all sides and the box was solvated using SPC/E water. The initial charge of the system was neutralized by adding counter ions of Na^+ and Cl^-. The salt concentration was set to 150 mM to mimic the physiological ion concentration. To remove any steric clashes, all the molecular systems were energy minimized using the steepest descent algorithm. The system was equilibrated under NVT (constant Number of particles, Volume, and Temperature) conditions for 100 ps at 300 K using the Berendsen thermostat and followed by NPT (constant

Number of particles, Pressure, and Temperature) condition pressure was equilibrated for 100 ps to 1 atm using the Berendsen barostat. During both the equilibrations, all the heavy atoms of the proteins were position restrained with a force constant of 1000 kJ $mol^{-1}nm^{-2}$. E_{pot} should be negative, and on the order of 10^5-10^6, depending on the system size and number of water molecules. Energy minimization gave us a reasonable starting structure, in terms of geometry and solvent orientation. Electrostatic interactions were calculated using Particle Mesh Ewald (PME) formalism. Equilibration of the solvent and ions around protein was done to begin molecular dynamics. A position restraining force can permit the movement of the heavy atoms of the protein except hydrogen atom, but only after overcoming a substantial energy penalty. The utility of position restraints is that they allow us to equilibrate our solvent around our protein, without the added variable of structural changes in the protein. Finally, 10 ns MD simulations were performed for each complex to analyze the stability of the system. The trajectory produced in MD simulation was analyzed using gmx rms, gmx rmsf, gmx gyrate, and gmx hbond of GROMACS utilities to obtain the root-mean-square deviation (RMSD), root-mean-square fluctuation (RMSF), the radius of gyration (R_g) and the number of H-bond s formed in EhSir2a. The differences in the energies like kinetic, potential, total, and pressure, and temperature were computed as a function of simulation time to check whether the systems obey NVT or NPT ensemble throughout the simulation. The trajectories were analyzed using the tools from GROMACS distribution. All the graphs were generated using the Grace tool (https://plasma-gate.weizmann.ac.il/Grace/).

RESULTS

Predicted interactors of EhSir2a

EhSir2a interacts with various proteins as found from STRING v11.0, to execute different types of molecular actions such as activation, inhibition, binding, phenotype, catalysis, post-translational modification, and gene expression. The interactors are predicted to be involved in the DNA repair pathway, chromosome structure maintenance, genome segregation, chromatin dynamics, transcription, and stress response. Some uncharacterized hypothetical proteins are also found as substrates of EhSir2a.

Zinc finger domain of EhSir2a

Bioinformatic analysis of EhSir2a showed that it has a unique N-terminal sequence of 134 amino acid residues in which a Zn-finger (ZnF) domain of 62 residues is embedded. The catalytic deacetylase domain is 240 amino acids long in EhSir2a. N-terminal part of EhSir2a is predominated by positively charged residues (Arginine and Lysine) and also unique as it is absent in other EhSir2 homologs. Zn-finger domain in EhSir2a is structured by five α-helices and one β-sheet but the crystallographic data showed the presence of two β-sheets and one α-helix in classical zinc-finger domain [62, 63] which indicates that ZnF in EhSir2a belongs to non-classical type where the position of cysteine/histidine combinations are very much different from currently approved 30 types of ZnF by the HUGO Gene Nomenclature Committee [62, 64].

Homology modeling

Homology modeling of EhSir2a and its interactors were built by using suitable templates and their quality was evaluated to determine the best stable model (Table-1).

Table-1: Template, quality estimation and evaluation of selected model of EhSir2a and its interactors using RAMPAGE: Assessment of the Ramachandran Plot, ProQ (Protein Quality Prediction), ResProx (Resolution-by-proxy), QMEAN4 score and ProSA

Parameters			Name of Proteins				
			EhSir2a	EhAT1	EhAT2	EhEF2	EhPBST3
Name of the template			4RMH	5UBQ, 5IYZ	5UBQ, 5IYZ	3J7P	5LE5, 5T0H
Quality Estimation Tools	RAMPAGE (Ramachandran plot)	Number of residues in favoured region	99.5%	98.5%	98.0%	97.0%	96.0%
		Number of residues in allowed region	0.5%	0.7%	1.3%	2.3%	4.0%
		Number of residues in outlier region	0.0%	0.9%	0.7%	0.7%	0.0%
	ProQ	LG score	2.914	4.566	4.509	4.772	3.960
		MaxSub	0.197	0.353	0.365	0.279	0.302
	ResProx Value		1.766	1.656	1.803	1.946	1.853
	QMEAN4 value		-1.93	-1.98	-2.08	-0.76	-0.26
	All Atom		-1.14	-0.30	-0.15	-0.43	0.37
	Cβ		-1.43	-1.32	-0.90	-1.31	-1.15
	Solvation		0.93	0.76	1.07	1.22	0.38
	Torsion		-1.88	-2.07	-2.36	-0.91	-0.19
	ProSA (Overall model quality in Z-score)		-5.72	-10.03	-10.17	-12.66	-8.78

All the PDB coordinate data in each of the modeled protein structures have been predicted with atomic resolution below 2Å whereas, a typical crystallographic model based on 2.0 Å data has a coordinate error of less than 0.2 Å. Resolution below 2 Å suggests that the structural quality of protein models was built with fewer systematic errors (such as missing or misplaced atoms) and with a less average coordinate error. Predicted QMEAN Z-score of modeled protein structures suggests that the 'degree of nativeness' or calculated secondary structure matched with the expected values from a representative set of high-resolution experimental structures. LG score and MaxSub values predicted by ProQ for the modeled proteins are near or above 3.0 and 0.1 proposed that structural quality is satisfactory for the theoretical model. Predicted Ramachandran plot of modeled protein structures showed above 95% of the amino acid residues fall into the favoured region, which indicates that theoretical conformations of protein have very less amount of steric hindrance or clashes between atoms with an acceptable range of phi and psi angles. ProSA predicts that the overall structural quality of the modeled proteins has a similar score as native proteins of the same residue obtained from X-ray analysis, NMR spectroscopy, and theoretical calculations. The best stable structured protein model of EhSir2a, EhAT1, EhAT2, EhEF2 and EhPBST3 were deposited in Protein Model DataBase (https://bioinformatics.cineca.it/PMDB/) as EhSir2a.pdb (PMDB id: PM0081615), EhAT1 (PMDB id: PM0082260), EhAT2 (PMDB id: PM0082261), EhEF2 (PMDB id: PM0082262) and EhPBST3 (PMDB id: PM0082264).

Structural analysis of EhSir2a and its interactors

The tertiary structure of modeled EhSir2a showed the presence of 6 parallel and 3 antiparallel β-sheets, 3 β-α-β units, 1 β-hairpin, 3 β-bulges (one parallel classic, one antiparallel G1 and one antiparallel special), 24 α-helices, 23 helix-helix interactions and 34 β-turns (Figure-1).

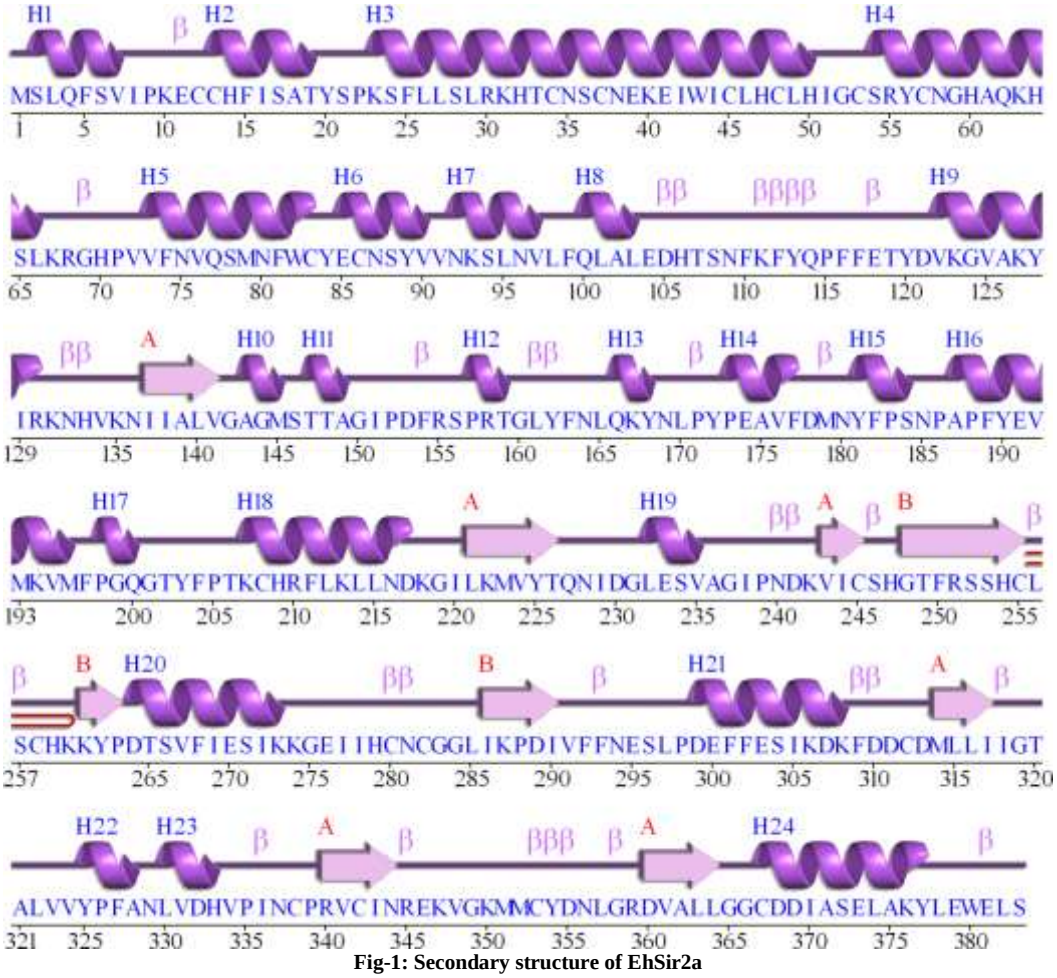

Fig-1: Secondary structure of EhSir2a

Theoretically designed structure of EhAT1 have 23 α-helices, 12 β-strands (10 mixed type and 2 antiparallel type), 5 β-α-β units, 1 β-hairpin, 1 ψ-loop, 2 β-bulges (one parallel classic and one antiparallel classic type), 26 helix-helix interactions, 33 β-turns, 9 γ-turns (one classic type and 8 inverse type) (Supplementary Figure-1).

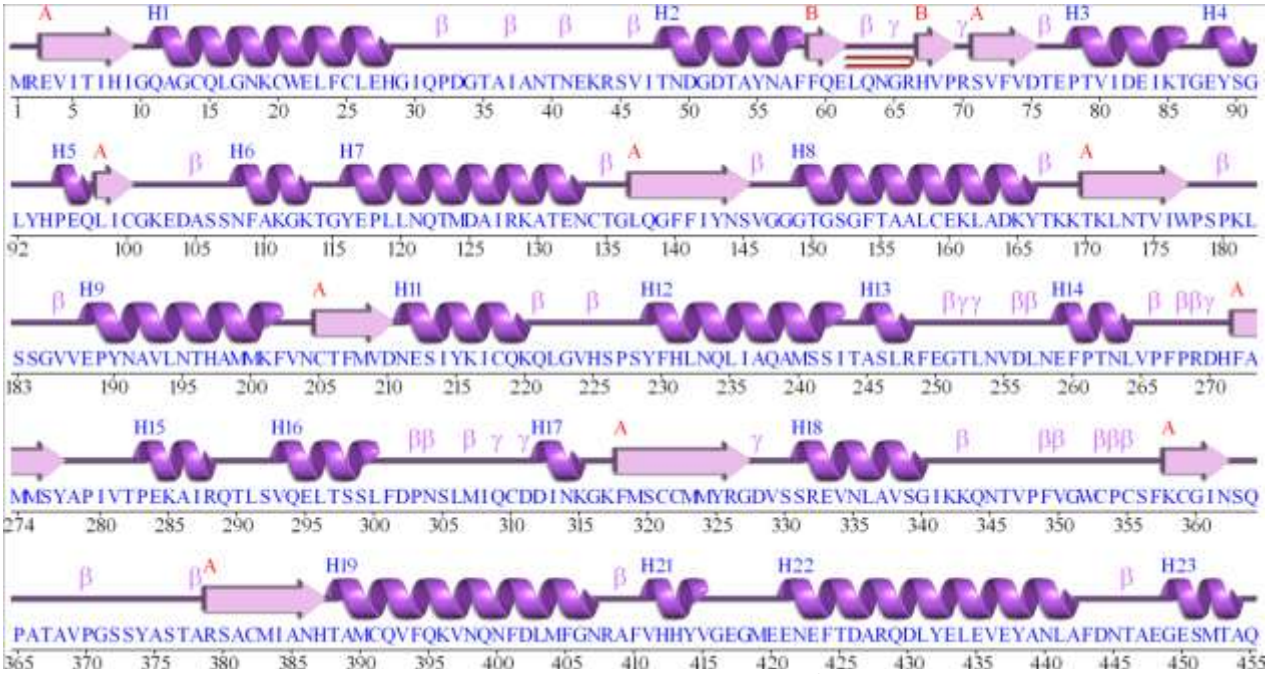

Supplementary Figure-1: Secondary structure of EhAT1

Structurally, EhAT2 is composed of 22 α-helices, 12 β-strands (10 mixed type and 2 antiparallel type), 5β-α-β units, 1 β-hairpin, 1 ψ-loop, 2 β-bulges (one parallel classic and one antiparallel classic type), 20 helix-helix interactions, 31 β-turns, 8 γ-turns (two classic type and 6 inverse type) (Supplementary Figure-2).

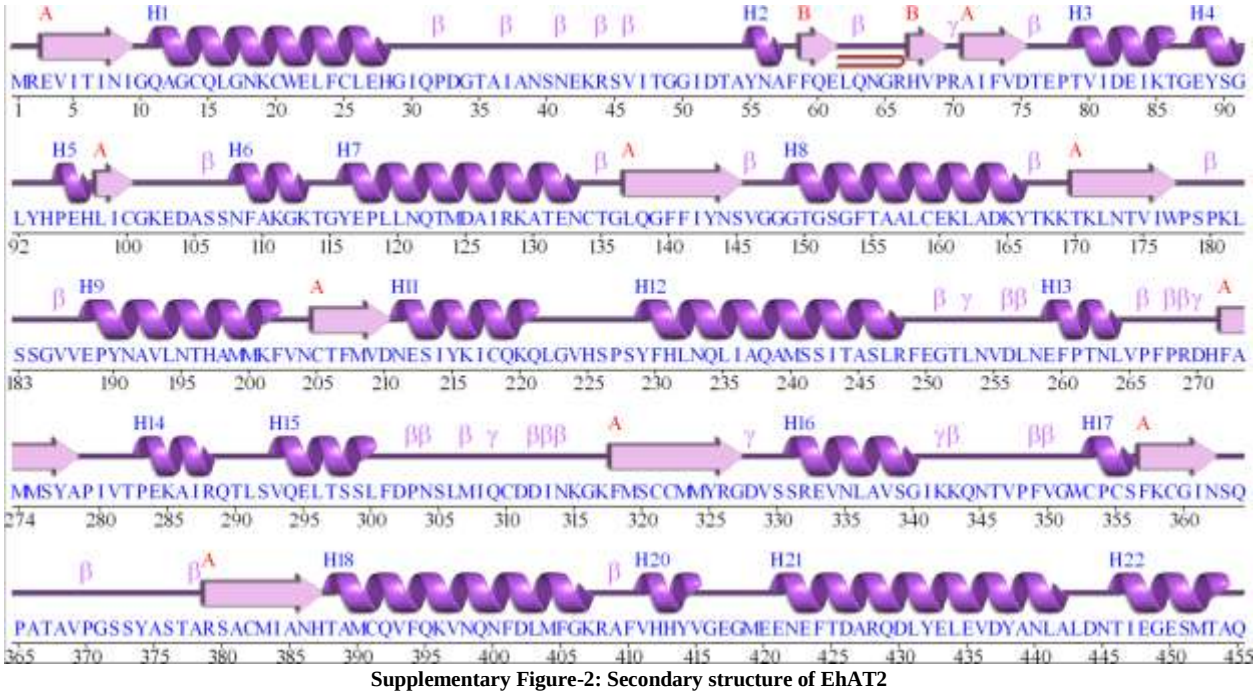

Supplementary Figure-2: Secondary structure of EhAT2

EhEF2 protein structure is contributed by 31 α-helices, 35 β-strands (12 mixed type and 23 antiparallel type), 3 β-α-β units, 10 β-hairpins, 1 ψ-loop, 11 β-bulges (one special antiparallel type, four G1 antiparallel type and six classic antiparallel type), 33 helix-helix interactions, 68 β-turns and 8 γ-turns (two classic type and six inverse type) (Supplementary Figure-3).

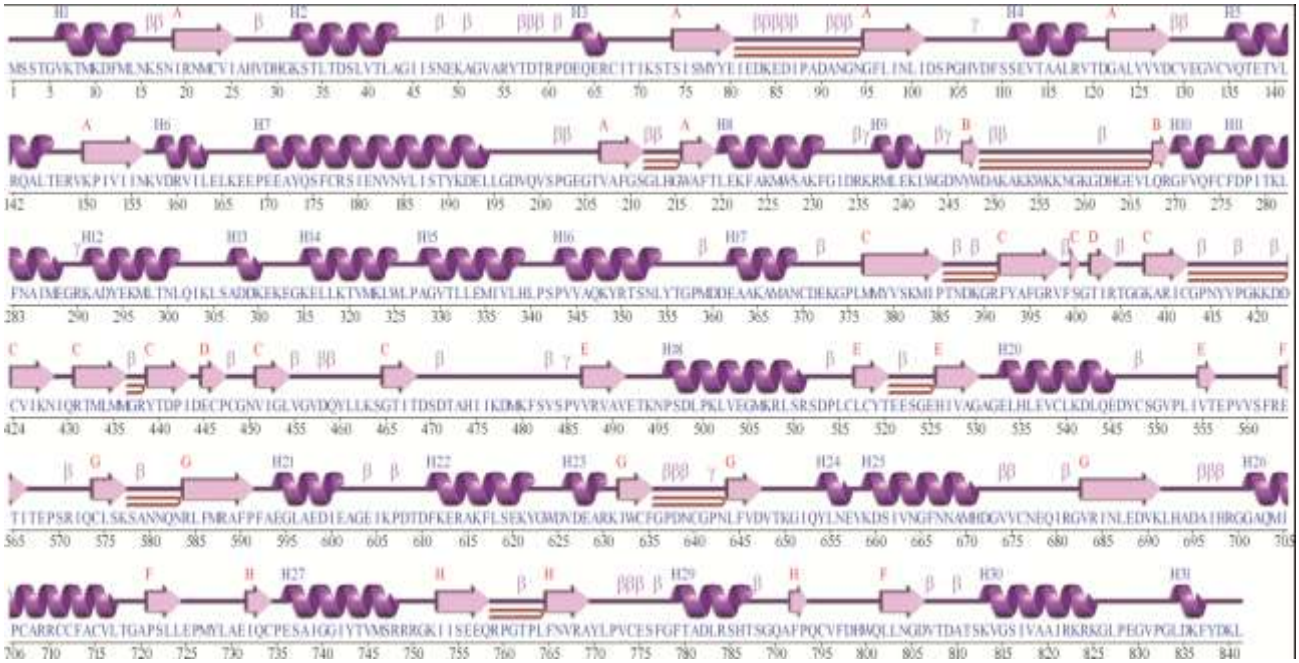

Supplementary Figure-3: Secondary structure of EhEF2

Structurally, EhPBST3 has 5 α-helices, 7 β-hairpins, 3 β-bulges (one classic antiparallel and two antiparallel G1 type), 12 antiparallel β-strands, 2 helix-helix interactions, 13 β-turns and 1 inverse type γ-turn (Supplementary Figure-4).

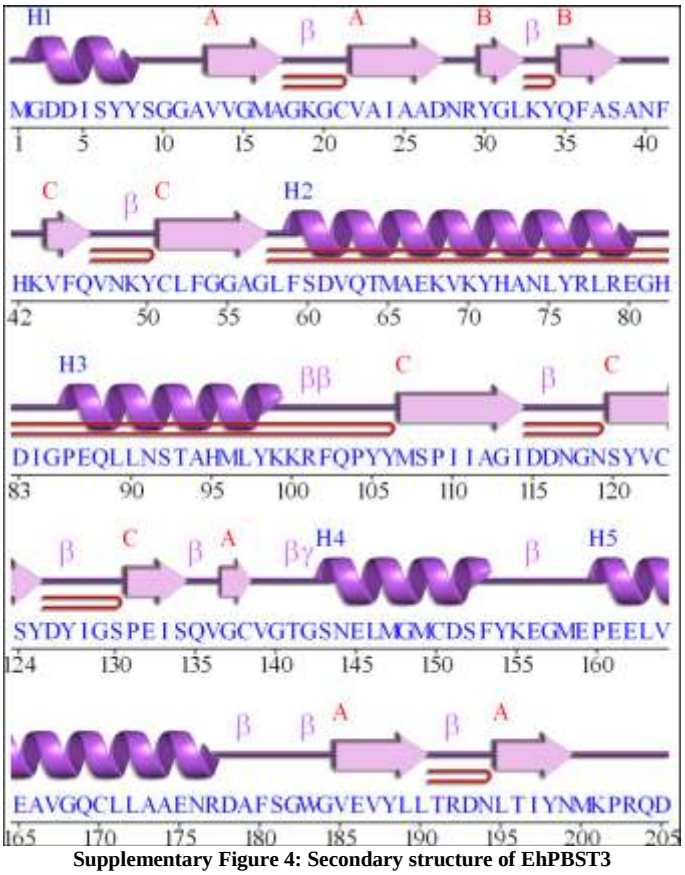

Supplementary Figure 4: Secondary structure of EhPBST3

Molecular interaction of EhSir2a with its interactors

Molecular Docking study was executed using the ClusPro v2.0 protein-protein molecular docking program. Among the four types of interaction modes, a balanced form of interaction was visualized by PyMOL (Table-2).

Table-2: Molecular Docking of EhSir2a with its interactors using ClusPro v2.0

	ClusPro v2.0											
	Balanced			Electrostatic-favored			Hydrophobic-favored			VdW+Elec		
	Members	Representative	Weighted Score	Members	Representative	Weighted Score	Members	Representative	Weighted Score	Members	Representative	Weighted Score
EhSir2a + EhAT1	66	Center	-848.6	71	Center	-924.9	140	Center	-1248.2	130	Center	-246.2
		Lowest Energy	-985.2		Lowest Energy	-1093.4		Lowest Energy	-1248.2		Lowest Energy	-301.4
EhSir2a + EhAT2	48	Center	-986.2	49	Center	-1086.4	61	Center	-1034.3	126	Center	-256.0
		Lowest Energy	-1083.7		Lowest Energy	-1086.4		Lowest Energy	-1217.7		Lowest Energy	-306.1
EhSir2a + EhEF2	58	Center	-901.0	51	Center	-965.2	145	Center	-994.8	58	Center	-269.4
		Lowest Energy	-1088.4		Lowest Energy	-1184.2		Lowest Energy	-1368.4		Lowest Energy	-308.2
EhSir2a + EhPBST3	89	Center	-859.5	62	Center	-892.3	119	Center	-1155.3	238	Center	-270.2
		Lowest Energy	-1044.8		Lowest Energy	-1059.2		Lowest Energy	-1387.9		Lowest Energy	-282.9

We further analyzed the docked conformation to find out the binding mode of interaction between the EhSir2a-EhSir2a interactor complex. Although the hydrophobic interactions are greatly responsible but comparative analysis of protein-protein interaction study with the HawkDock server showed hydrogen bonds are also necessary to stabilize the interaction between the proteins. Interaction study of EhSir2a with EhAT1, EhAT2, EhEF2, and EhPBST3 was carried out by HawkDock evaluated lowest free energy of binding were -54.46 Kcal.mol^{-1}, -47.21 Kcal.mol^{-1}, -41.99 Kcal.mol^{-1} and -46.38 Kcal.mol^{-1} respectively (Table-3).

Table-3: Structural prediction and analysis of protein-protein complex of EhSir2a and its interactors using HawkDock server

	HawkDock Server		No. of H-bonds	Residues involved in H-bond interaction		Bond length (Å)	Residues involved in hydrophobic contacts	
	HawkDock Score	MM/GBSA Binding free energy of complex		EhSir2a (B)	EhSir2a interactor (A)		EhSir2a (B)	EhSir2a interactor (A)
EhSir2a + EhAT1	-4861.48	-54.46 kcal/mol	9	(Tyr203)O	(Arg269)NH1	3.01	Phe204, Leu214, Lys213, Pro205, Val235, Asn240, Ile238, Ser234, Lys261, Pro263, Asp264, Arg251	Lys201, Phe267, Phe405, Arg408, Arg428, Asp430, Tyr432, Gly449, Glu450, Met452, Ala454
				(Glu381)OE2	(Asn422)ND2	2.81		
				(Glu381)O	(Thr425)OG1	2.97		
				(Leu382)O	(Thr425)OG1	1.53		
				(Ser383)O	(Gln429)NE2	3.30		
				(Arg210)NH1	(Glu433)OE2	2.63		
				(Arg210)NH2	(Glu433)OE2	2.45		
				(Thr265)N	(Thr453)O	2.98		
				(Thr265)N	(Gln455)O	2.85		
EhSir2a + EhAT2	-5059.60	-47.21 kcal/mol	5	(Asn92)OD1	(Lys315)NZ	2.70	Lys93, Asn96, Val97, Thr107, Leu101, His106, Thr33, Lys111, Ser108, Phe112, Phe99, Asn80, Leu98	Asn314, Lys317, Gln395, Gln399, Phe405, Gln429, Tyr432, Glu435, Val436, Ala439, Asn440, Ala442, Leu443
				(Glu41)OE2	(Arg408)NH1	3.13		
				(Asn109)OD1	(Asn398)ND2	2.29		
				(Cys37) SG	(Asn422)OD1	2.28		
				(Asn109)O	(Arg428)NH1	2.11		

EhSir2a + EhEF2	-4707.73	-41.99 kcal/mol	7	(Lys350)NZ	(Glu168)OE1	3.08	Pro71, His70, Leu364, Ala18, Tyr20, Ser21, Leu98, Val97, Ser94, Val91, Asn87, Tyr84, Met79	Val130, Glu131, Leu165, Gly264, Ser737, Ile739, Gly740, Gly741, Tyr743, Thr744, His786, Thr787
				(Lys347)NZ	(Lys166)O	3.29		
				(Lys347)NZ	(Glu168)OE1	2.30		
				(Asn356)ND2	(Glu171)OE2	2.25		
				(Thr19)O	(Lys260)NZ	2.21		
				(Cys83)SG	(Ser785)O	3.16		
				(Asn80)OD1	(Ser788)OG	2.31		
EhSir2a + EhPBST3	-5597.87	-46.38 kcal/mol	5	(Asn356)ND2	(Asp151)OD2	3.10	Lys350, Phe25, Lys111, Pro22, Cys353, Phe74, Val72, Val73, Val76, Cys12, Ala18, Tyr20, Thr19, Phe15, Phe99	Met147, Ser143, Ser130, Arg177, Ile128, Ile133, Leu90, Asp178, Glu87, Tyr7, Phe180, Lys33, Asn91
				(Met352)CE	(Asn144)ND2	3.18		
				(Lys10)LZ	(Asp4)OD1	2.94		
				(Pro71)O	(Gln135)NE2	2.51		
				(His14)O	(Tyr34)OH	2.92		

Alpha-tubulin conserved domain of both EhAT1 and EhAT2 have following nucleotide-binding sites at R2, Q11, A12, Q15, E77, P78, T79, S106, S107, N108, K111, G148, G149, T150, G151, I176, V186, E188, N204, N211, Y229, N233. Interaction analysis of both α-tubulin proteins with EhSir2a showed that hydroxyl amino acids and acidic amino acids are essential for the formation of H-bonds. Tyr432, Asn422, Arg408 residues of EhAT1, and EhAT2 are common in interaction with Ehsir2a. This implies that Tyr432, Asn422, Arg408 of α-tubulin are essential for interaction with EhSir2a (Figure-2, Supplementary Figure 5-8). The molecular interaction of EhSir2a with its interacting proteins is shown in Figure-3.

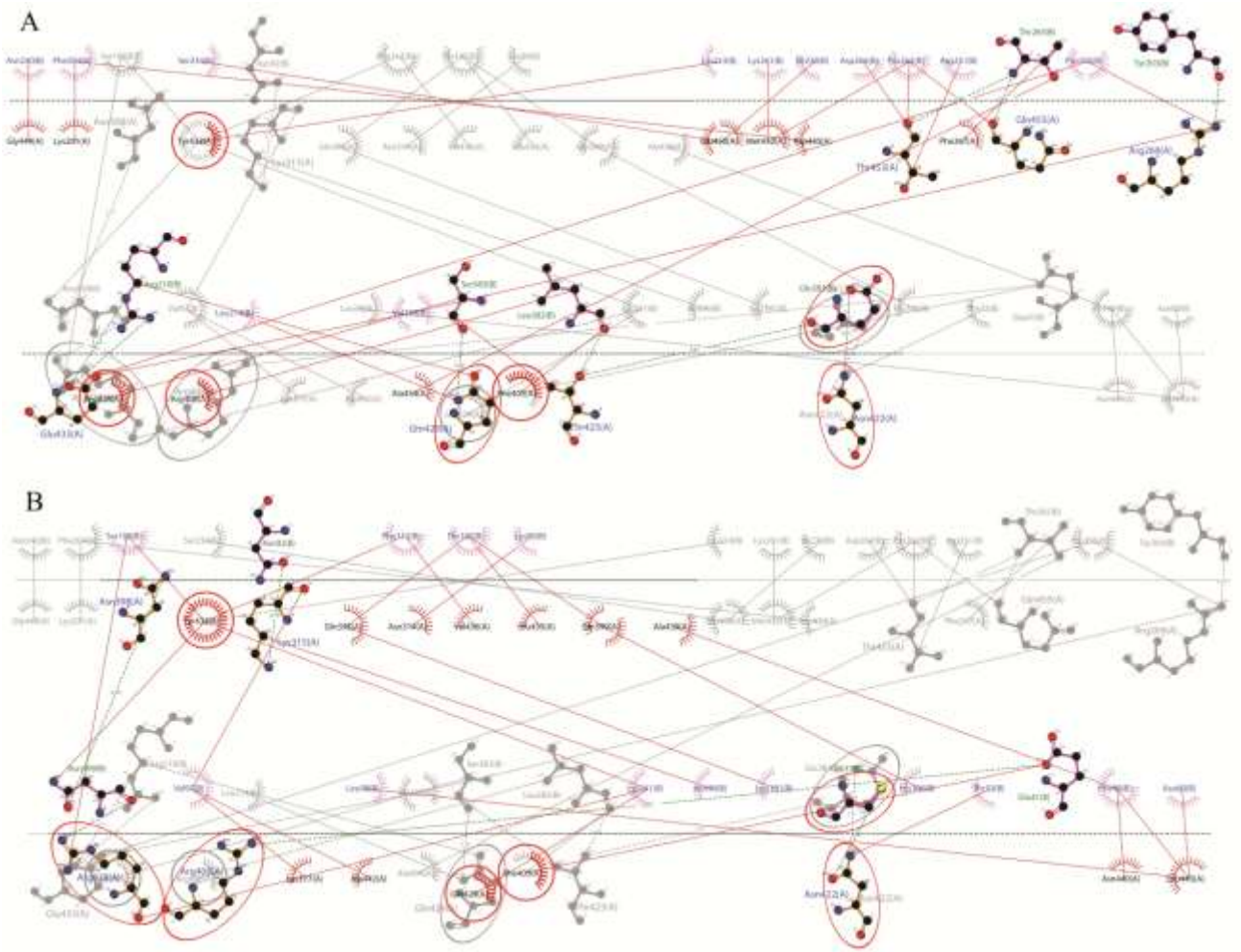

Fig-2: Merged representation of molecular interactions between EhSir2a and two isoforms of α-tubulin, EhAT1 and EhAT2. (A) Interaction with EhAT1 is actively highlighted (B) Interaction with EhAT2 is actively highlighted. Encircled amino acids are common residues involved in interaction with EhSir2a with both the isoform of Eh α-tubulin

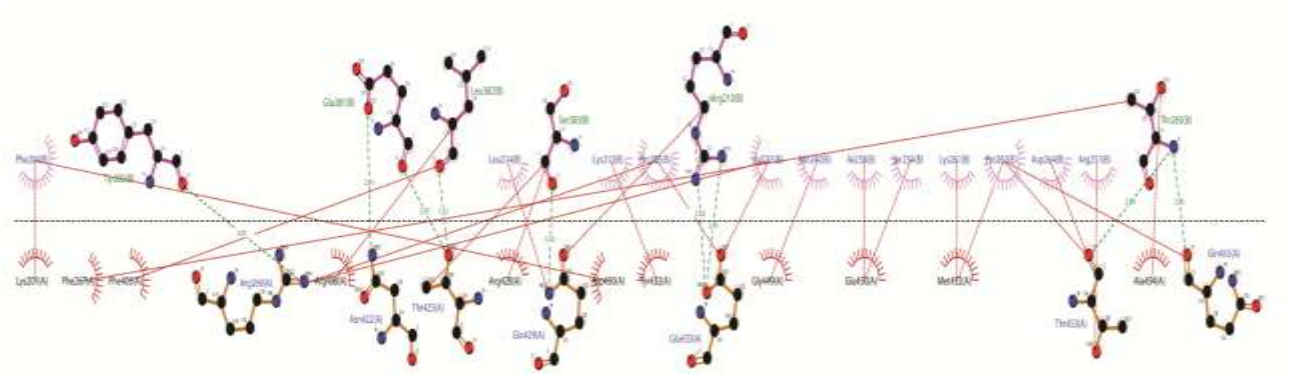

Supplementary Figure-5: Schematic representation of the molecular interactions between EhSir2a and EhAT1. Amino acids of EhSir2a (B) (pink coloured arc) involved in hydrophobic contacts with amino acids of EhAT1 (A) (red coloured arc) are indicated by an arc with spokes radiating towards each other. The atoms of amino acids involved in hydrophobic interaction have small red spokes on them. The horizontal black dash line represents the interface. The green coloured dash line indicates the hydrogen bond between corresponding atoms with its bond length

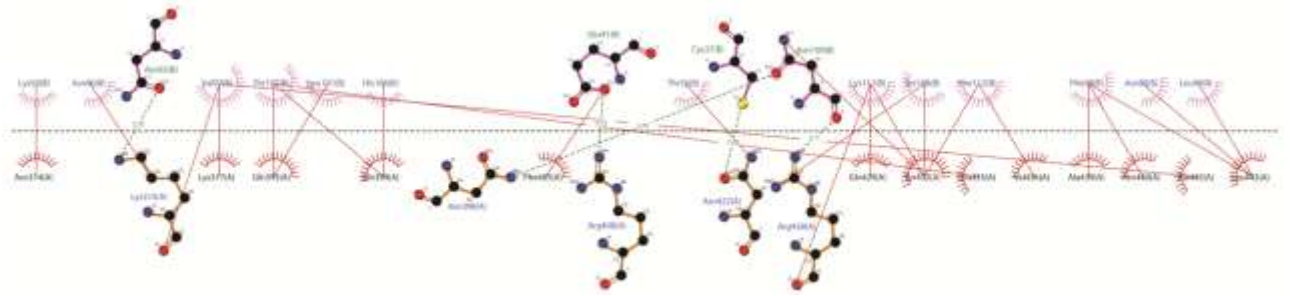

Supplementary Figure-6: Schematic representation of the molecular interactions between EhSir2a and EhAT2. Amino acids of EhSir2a (B) (pink coloured arc) involved in hydrophobic contacts with amino acids of EhAT2 (A) (red coloured arc) are indicated by an arc with spokes radiating towards each other. The atoms of amino acids involved in hydrophobic interaction have small red spokes on them. The horizontal black dash line represents the interface. The green coloured dash line indicates the hydrogen bond between corresponding atoms with its bond length

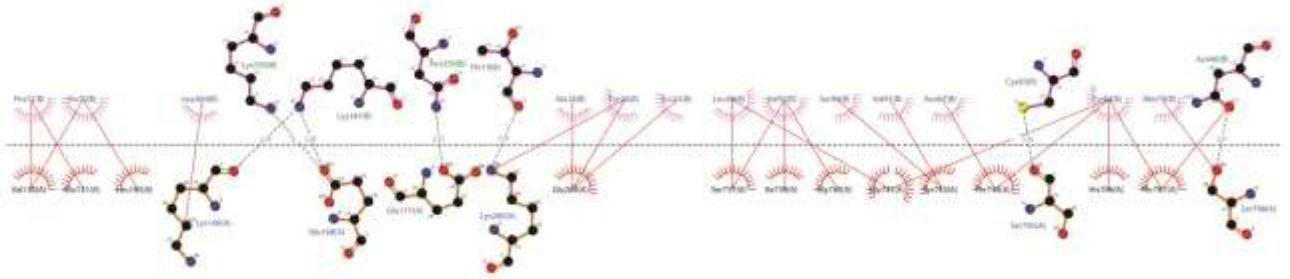

Supplementary Figure-7: Schematic representation of the molecular interactions between EhSir2a and EhEF2. Amino acids of EhSir2a (B) (pink coloured arc) involved in hydrophobic contacts with amino acids of EhEF2 (A) (red coloured arc) are indicated by an arc with spokes radiating towards each other. The atoms of amino acids involved in hydrophobic interaction have small red spokes on them. The horizontal black dash line represents the interface. The green coloured dash line indicates the hydrogen bond between corresponding atoms with its bond length

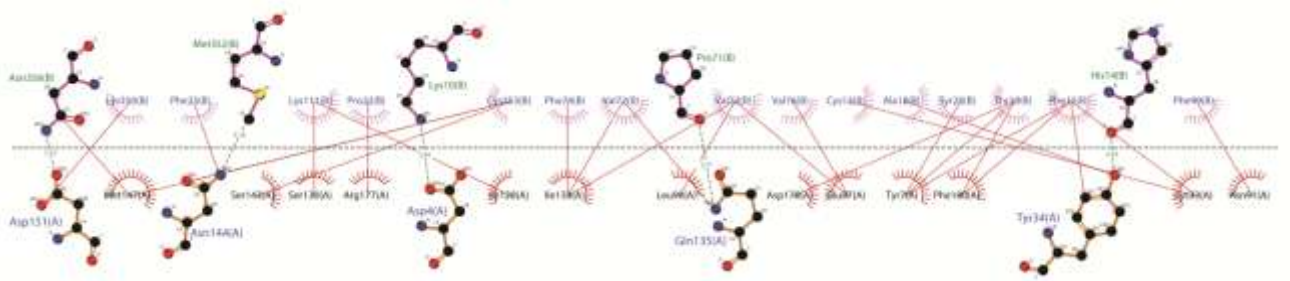

Supplementary Figure-8: Schematic representation of the molecular interactions between EhSir2a and EhPBST3. Amino acids of EhSir2a (B) (pink coloured arc) involved in hydrophobic contacts with amino acids of EhPBST3 (A) (red coloured arc) are indicated by an arc with spokes radiating towards each other. The atoms of amino acids involved in hydrophobic interaction have small red spokes on them. The horizontal black dash line represents the interface. The green coloured dash line indicates the hydrogen bond between corresponding atoms with its bond length

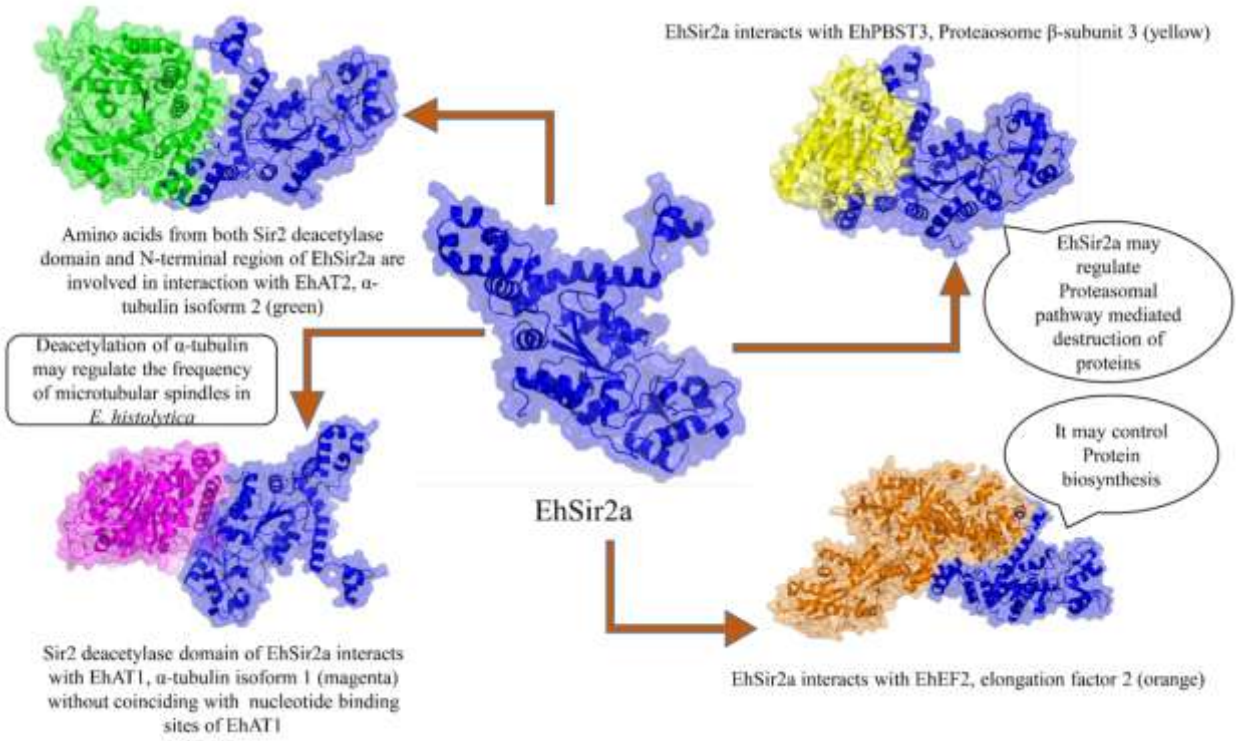

Fig-3: Schematic representation of EhSir2a with its interactors.

MD simulation of EhSir2a

Energy minimization (EM) of EhSir2a protein was conducted using SPC/E water in a cubic box with GROMOS96 54a7 force field at 300 K. Initially, the system had a non-zero total charge 2.999998 but it was neutralized by adding three Cl^- ions and the potential energy was 2.40702 x10^5 kJ mol^{-1}. EM was achieved in 499 steps by steepest descent method with a final minimized energy of -4.32909 x 10^5 kJ mol^{-1} with an average value of -4.01012 x 10^5 kJ mol^{-1} (Figure-4).

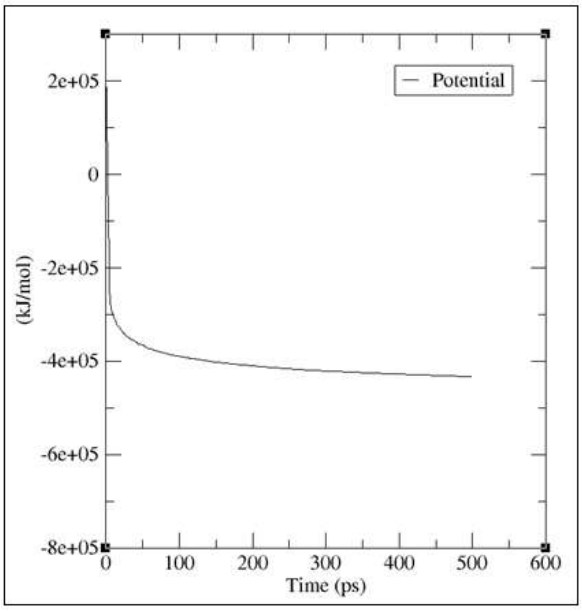

Fig-4: Energy minimization curve of EhSir2a model structure by steepest descent method showed a decline in potential energy and remained constant after 499 steps with the potential energy of -4.32909 x 10^5 KJ.mol^{-1}

This value is significant for a satisfactory EM. After the NVT ensemble, the average temperature of this energy minimized protein in the system was recorded as 299.971 K, which is very much close to 300 K states that molecular simulation didn't collapse because of the flexibility of this protein model (Supplementary Figure-9).

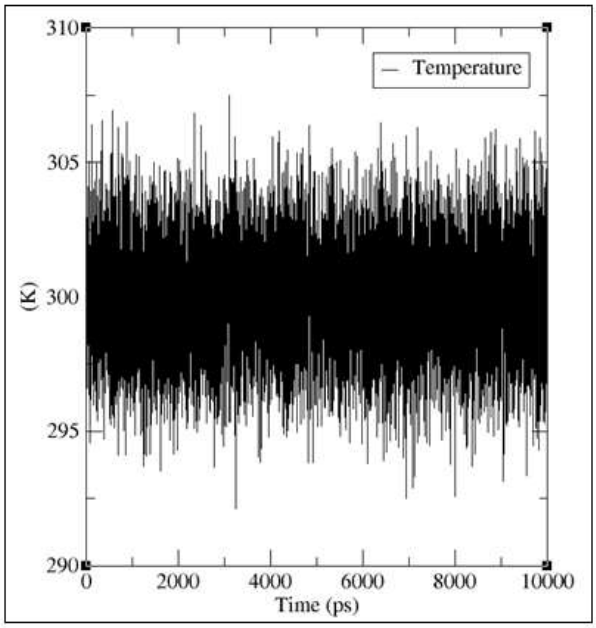

Supplementary Figure-9: Temperature curve of EhSir2a model structure showed a rise in system temperature, becoming stable at 300 K with a running average of 299.971 K. Significant at P < 0.001, i.e., the system is well equilibrated in terms of temperature

After the NPT ensemble, the average pressure and density were recorded as 1.64519 bar and 1062.07 Kg m^{-3} (Supplementary Figure 10, 11), respectively which suggest that the system reached the equilibrium and stabilized in terms of density and pressure within nanosecond time scale.

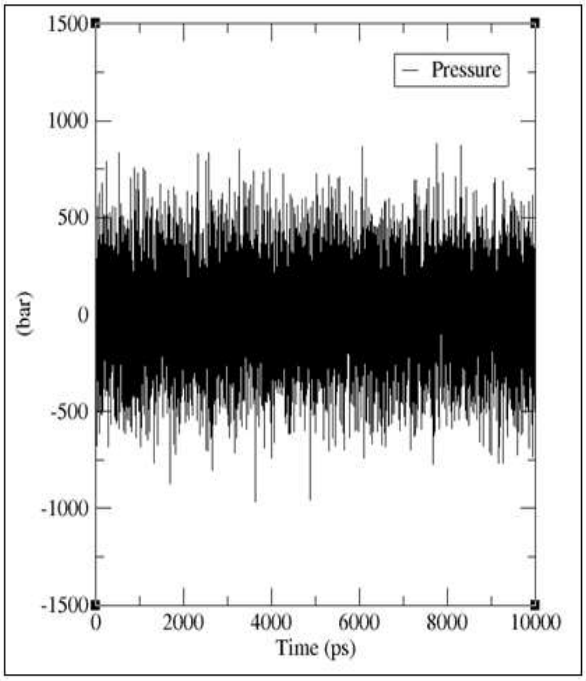

Supplementary Figure-10: Pressure curve of EhSir2a model structure at 300 K showed an average pressure of 1.64519 bar

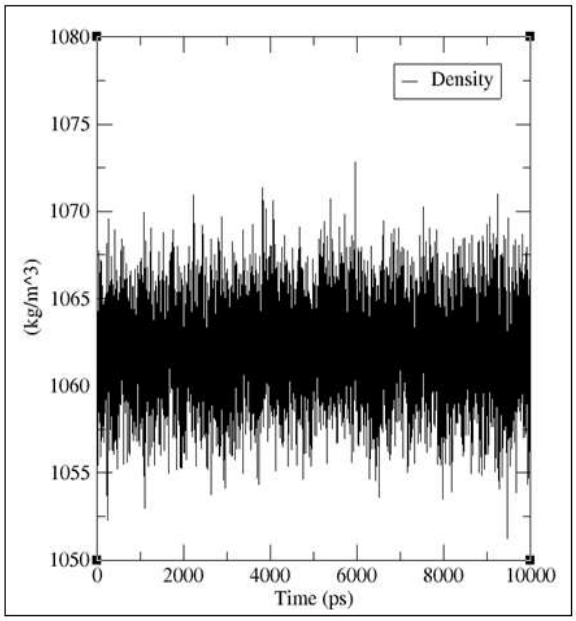

Supplementary Figure-11: Density curve of EhSir2a model structure at 300 K showed an average density of 1062.07 kg m^{-3}

The structural stability of the designed model of EhSir2a was run through 10 ns of MD simulation followed by the analysis of RMSD, RMSF, R_g, H-bonds to obtain a better picture of structural properties in aqueous condition having physiological salt concentration. MD trajectories of EhSir2a used to analyze the RMSD of the protein backbone atoms as a function of time (Supplementary Figure-12).

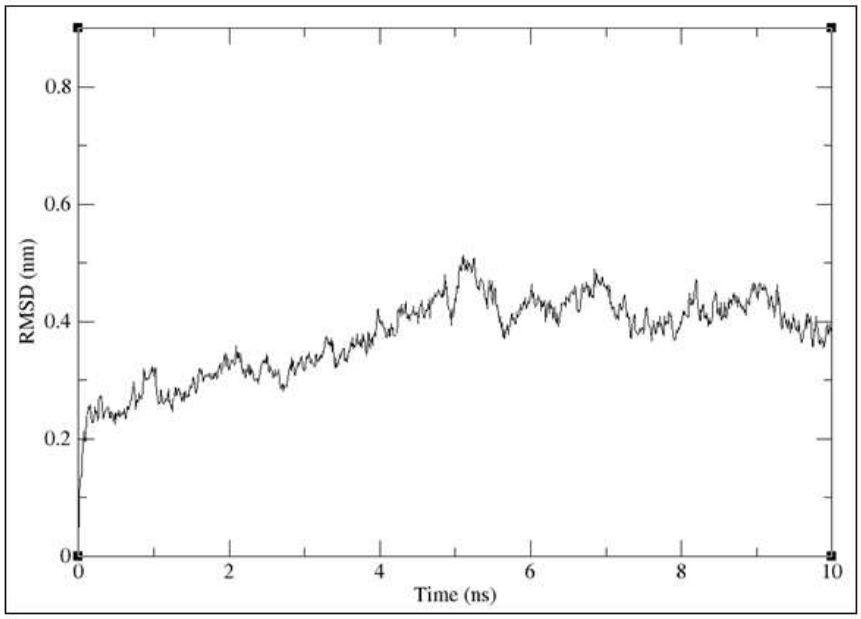

Supplementary Figure-12: RMSD of EhSir2a backbone structure over 10 ns

From this figure, it can be observed that the RMSD value within 0.1-0.5 during the 0-10 ns time scale. Initially, the RMSD value is increased up to 0.5 within 5 ns but after that, no further increment in RMSD value suggests that EhSir2a reaches an equilibrium state. The RMSF study of EhSir2a MD simulation is used to analyze the flexibility of the backbone structure (Supplementary Figure 13).

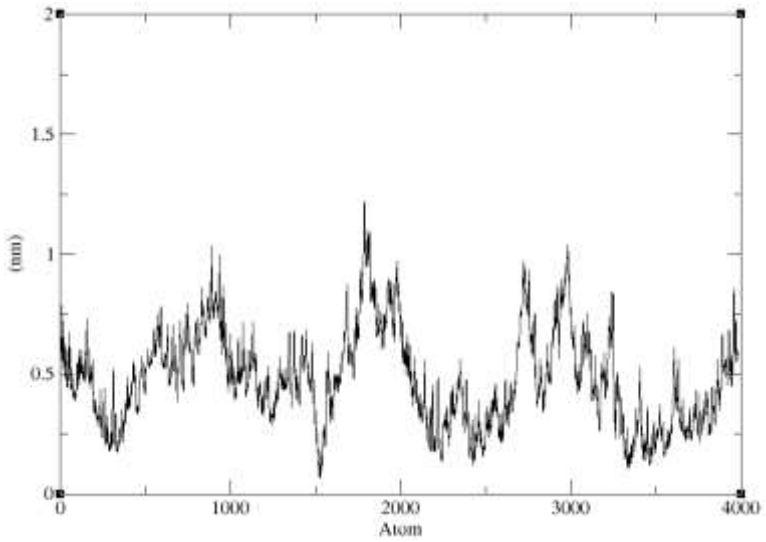

Supplementary Figure-13: RMSF showed the fluctuation of each atoms in amino acid residue of EhSir2a

The RMSF of the atoms in residues in the active site of the ZnF domain and Sir2 domain EhSir2a show more fluctuation during simulation from its average position, indicate the flexibility and accessibility of the region for its interactor proteins. The low RMSF value indicates limited movements during simulation to its average position. This suggests that these atoms belong to the amino acid residues which are rigid due to chemical bonds. From the R_g plot, we can determine the compaction level in EhSir2a. The R_g value of EhSir2a varies between 2.5-2.6 nm which reveals the stability of EhSir2a designed structure in simulated biological conditions over a 10 ns time scale (Supplementary Figure-14).

a

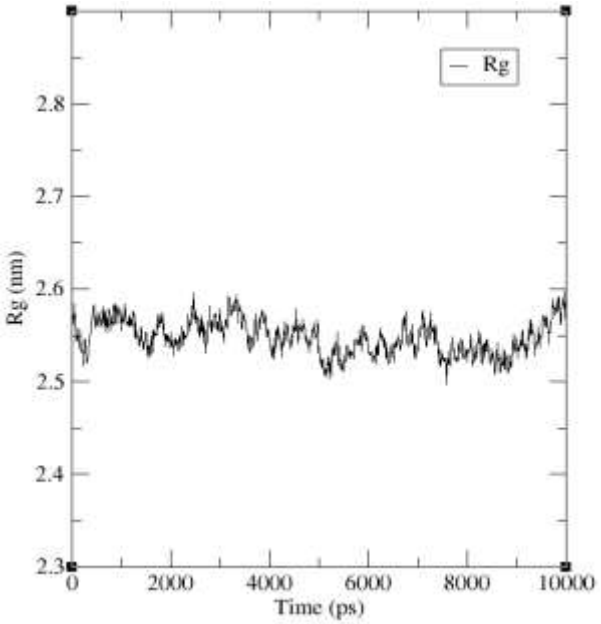

Supplementary Figure-14: The radius of gyration of EhSir2a over 10,000 ps time frame showed the compactness of structure

In a 10 ns simulation time, hydrogen bonds with both intermolecular level (Supplementary Figure-15) and solvent molecule (Supplementary Figure-16) suggest its stability of protein structural conformation.

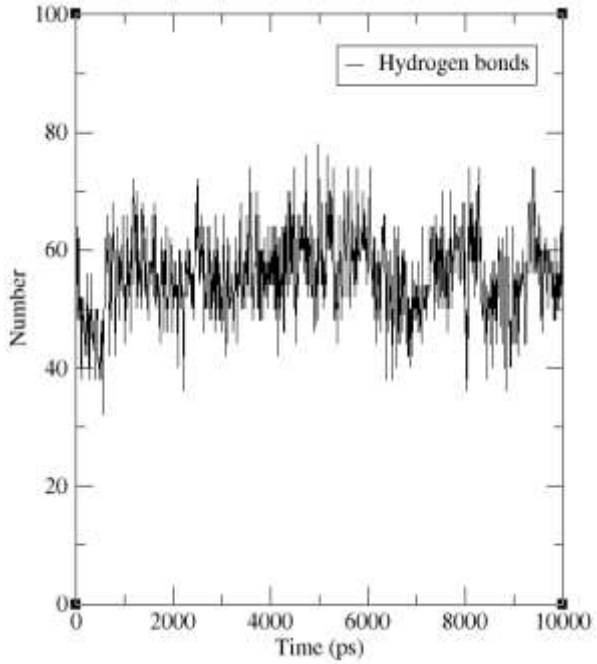

Supplementary Figure-15: Number of hydrogen bonds in EhSir2a at intermolecular level fluctuate initially but achieved equilibrium within nanosecond time scale

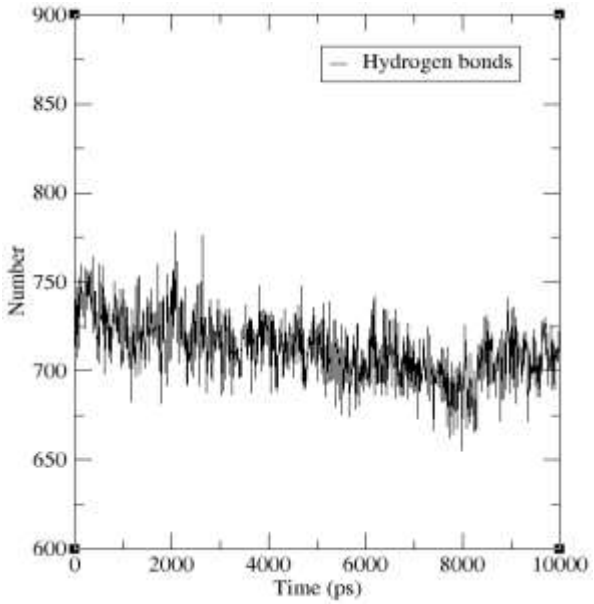

Supplementary Figure-16: Number of hydrogen bonds in EhSir2a with solvent molecule gradually decrease with time and reached equilibrium within nanosecond time scale

DISCUSSION

From a previous study, we have identified the interactors of EhSir2a by yeast two-hybrid genetic screening against the cDNA library of *E. histolytica* and identified their probable biological role in this parasite [19]. This study shows the detailed molecular interactions occurring between EhSir2a and its interacting proteins that are identified from the experimental method or by STRING analysis. Few interactors are not found by STRING analysis even at a confidence level of 0.4 but identified by cDNA library screening. This may be because *E. histolytica* being a protozoan parasite behaves differently than model organisms. Zinc finger domain-containing proteins are extremely abundant in eukaryotic genomes. It has versatile functions which include DNA binding, RNA packaging, transcriptional activation, regulation of apoptosis, protein folding and assembly, protein-protein, and protein-lipid interactions [65-70]. The Zn finger domain of EhSir2a is different from the other 30 types of zinc-finger domain found in higher eukaryotes. According to NCBI conserve domain search analysis, EhSir2a-ZnF is closely related to Zn-finger in ubiquitin-hydrolases (zf-UBP, Acc. Id: pfam02148). The Zn finger domain present at the N-terminal part of EhSir2a is probably responsible for its interaction with chromatin and other proteins. The RMSF of the atoms in the amino acid residues present in the active site of the ZnF domain and Sir2 domain of EhSir2a show more fluctuation during the simulation as compared to its average position. This indicates the flexibility and accessibility of the region for its interactor proteins. The low RMSF value indicates limited movements during simulation concerning its average position suggesting these atoms belong to the amino acid residues which are rigid. We have studied the molecular interaction between EhSir2a with its interactor EhAT1 and found that interacting site is different from the nucleotide-binding sites of EhAT1. Both EhAT1 and EhAT2 interact with the deacetylase domain of EhSir2a. The interaction of EhAT2 is different in the sense that it interacts with the N terminus of EhSir2a also, where EhAT1 has not any.

CONCLUSION

The molecular interaction between EhSir2a and EhAT1 with the low free energy of binding suggests the stable interaction between them in the intercellular environment. Several proteins with diverse functionality predicted to be the interactors of EhSir2a indicates that it is involved in different cellular functions. The presence of positive amino acids in the zinc finger domain in EhSir2a may interact with specific sites on DNA and again, this may be the reason for interaction with an elongation factor, EhEF2. Various intercellular localization of EhSir2a and stable interaction with proteasome beta type3 domain-containing protein, EhPBST3 suggests its role in controlling the degradation of non-lysosomal protein in cytosol and nucleus. The intercellular concentration of regulatory protein works as a sensor of cellular cell cycle phase and metabolic state. The concentration of these regulatory proteins orchestrates with a function of time by degradation via the proteasomal pathway. From this study, it can be concluded that EhSir2a, a sirtuin homolog from the human parasite may have some novel functions that are not associated with sirtuins from other organisms.

DECLARATIONS

Ethics approval and consent to participate: Not applicable

Consent for publication: Not applicable

Availability of data and material: Not applicable

Competing interests: The authors declare that they have no conflict of interest.

Funding: DAE-BRNS project (37 (1)/20/15/2014-BRNS/808), 2014-2017

ACKNOWLEDGEMENTS

This study was supported by DAE-BRNS project (37 (1)/20/15/2014-BRNS/808), 2014-2017 to SD and PB was supported by State-funded fellowship, The University of Burdwan, West Bengal, India.

REFERENCES

1. Haque, R. (2007). Human intestinal parasites. *Journal of health, population, and nutrition*, *25*(4), 387-391.
2. Petri Jr, W. A., Haque, R., Lyerly, D., & Vines, R. R. (2000). Estimating the impact of amebiasis on health. *Parasitology Today*, *16*(8), 320-321.

3. Amoebiasis. (1997). Releve epidemiologique hebdomadaire. 72(14):97-99.
4. Das, S., & Lohia, A. (2002). Delinking of S phase and cytokinesis in the protozoan parasite Entamoeba histolytica. *Cellular Microbiology*, *4*(1), 55-60.
5. Mukherjee, C., Majumder, S., & Lohia, A. (2009). Inter-cellular variation in DNA content of Entamoeba histolytica originates from temporal and spatial uncoupling of cytokinesis from the nuclear cycle. *PLoS Negl Trop Dis*, *3*(4), e409.
6. Lohia, A., Mukherjee, C., Majumder, S., & Dastidar, P. G. (2007). Genome re-duplication and irregular segregation occur during the cell cycle of Entamoeba histolytica. *Bioscience reports*, *27*(6), 373-384.
7. Lohia, A. (2003). The cell cycle of Entamoeba histolytica. *Molecular and cellular biochemistry*, *253*(1-2), 217-222.
8. Banerjee, S., Das, S., & Lohia, A. (2002). Eukaryotic checkpoints are absent in the cell division cycle ofEntamoeba histolytica. *Journal of biosciences*, *27*(6), 567-572.
9. Mehlotra, R. K. (1996). Antioxidant defense mechanisms in parasitic protozoa. *Critical reviews in microbiology*, *22*(4), 295-314.
10. Tekwani, B. L., & Mehlotra, R. K. (1999). Molecular basis of defence against oxidative stress in Entamoeba histolytica and Giardia lamblia. *Microbes and infection*, *1*(5), 385-394.
11. Vassilopoulos, A., Fritz, K. S., Petersen, D. R., & Gius, D. (2011). The human sirtuin family: evolutionary divergences and functions. *Human genomics*, *5*(5), 1-12.
12. Greiss, S., & Gartner, A. (2009). Sirtuin/Sir2 phylogeny, evolutionary considerations and structural conservation. *Molecules and cells*, *28*(5), 407-415.
13. Bitterman, K. J., Anderson, R. M., Cohen, H. Y., Latorre-Esteves, M., & Sinclair, D. A. (2002). Inhibition of silencing and accelerated aging by nicotinamide, a putative negative regulator of yeast sir2 and human SIRT1. *Journal of Biological Chemistry*, *277*(47), 45099-45107.
14. Anderson, R. M., Bitterman, K. J., Wood, J. G., Medvedik, O., & Sinclair, D. A. (2003). Nicotinamide and PNC1 govern lifespan extension by calorie restriction in Saccharomyces cerevisiae. *Nature*, *423*(6936), 181-185.
15. Kustatscher, G., Hothorn, M., Pugieux, C., Scheffzek, K., & Ladurner, A. G. (2005). Splicing regulates NAD metabolite binding to histone macroH2A. *Nature structural & molecular biology*, *12*(7), 624-625.
16. Liou, G. G., Tanny, J. C., Kruger, R. G., Walz, T., & Moazed, D. (2005). Assembly of the SIR complex and its regulation by O-acetyl-ADP-ribose, a product of NAD-dependent histone deacetylation. *Cell*, *121*(4), 515-527.
17. Tong, L., & Denu, J. M. (2010). Function and metabolism of sirtuin metabolite O-acetyl-ADP-ribose. *Biochimica et Biophysica Acta (BBA)-Proteins and Proteomics*, *1804*(8), 1617-1625.
18. Houtkooper, R. H., Pirinen, E., & Auwerx, J. (2012). Sirtuins as regulators of metabolism and healthspan. *Nature reviews Molecular cell biology*, *13*(4), 225-238.
19. Dam, S., & Lohia, A. (2010). Entamoeba histolytica sirtuin EhSir2a deacetylates tubulin and regulates the number of microtubular assemblies during the cell cycle. *Cellular microbiology*, *12*(7), 1002-1014.
20. Merrick, C. J., Dzikowski, R., Imamura, H., Chuang, J., Deitsch, K., & Duraisingh, M. T. (2010). The effect of Plasmodium falciparum Sir2a histone deacetylase on clonal and longitudinal variation in expression of the var family of virulence genes. *International journal for parasitology*, *40*(1), 35-43.
21. Tonkin, C. J., Carret, C. K., Duraisingh, M. T., Voss, T. S., Ralph, S. A., Hommel, M., ... & Speed, T. P. (2009). Sir2 paralogues cooperate to regulate virulence genes and antigenic variation in Plasmodium falciparum. *PLoS Biol*, *7*(4), e1000084.
22. Baharia, R. K., Tandon, R., Sharma, T., Suthar, M. K., Das, S., Siddiqi, M. I., ... & Dube, A. (2015). Recombinant NAD-dependent SIR-2 protein of Leishmania donovani: immunobiochemical characterization as a potential vaccine against visceral leishmaniasis. *PLoS Negl Trop Dis*, *9*(3), e0003557.
23. Purkait, B., Singh, R., Wasnik, K., Das, S., Kumar, A., Paine, M., ... & Das, P. (2015). Up-regulation of silent information regulator 2 (Sir2) is associated with amphotericin B resistance in clinical isolates of Leishmania donovani. *Journal of Antimicrobial Chemotherapy*, *70*(5), 1343-1356.
24. Vergnes, B., Gazanion, E., & Grentzinger, T. (2016). Functional divergence of SIR2 orthologs between trypanosomatid parasites. *Molecular and biochemical parasitology*, *207*(2), 96-101.
25. Moreira, D., Rodrigues, V., Abengozar, M., Rivas, L., Rial, E., Laforge, M., ... & da Silva, A. C. (2015). Leishmania infantum modulates host macrophage mitochondrial metabolism by hijacking the SIRT1-AMPK axis. *PLoS Pathog*, *11*(3), e1004684.
26. Silvestre, R., Cordeiro- da- Silva, A., Tavares, J., Sereno, D., & Ouaissi, A. (2006). Leishmania cytosolic silent information regulatory protein 2 deacetylase induces murine B- cell differentiation and in vivo production of specific antibodies. *Immunology*, *119*(4), 529-540.
27. Silvestre, R., Cordeiro-Da-Silva, A., Santarém, N., Vergnes, B., Sereno, D., & Ouaissi, A. (2007). SIR2-deficient Leishmania infantum induces a defined IFN-γ/IL-10 pattern that correlates with

protection. *The Journal of Immunology*, *179*(5), 3161-3170.

28. Vergnes, B., Vanhille, L., Ouaissi, A., & Sereno, D. (2005). Stage-specific antileishmanial activity of an inhibitor of SIR2 histone deacetylase. *Acta tropica*, *94*(2), 107-115.
29. Fessel, M. R., Lira, C. B., Giorgio, S., Ramos, C. H. I., & Cano, M. I. N. (2011). Sir2-Related Protein 1 from Leishmania amazonensis is a glycosylated NAD (+)-dependent deacetylase. *Parasitology*, 1245-1258.
30. Dong, H., Yang, S., Zhao, Q., Han, H., Zhu, S., Zhu, X., ... & Yang, L. (2016). Molecular characterization and protective efficacy of silent information regulator 2A from Eimeria tenella. *Parasites & vectors*, *9*(1), 602.
31. Xie, H., Lei, N., Gong, A. Y., Chen, X. M., & Hu, G. (2014). Cryptosporidium parvum induces SIRT1 expression in host epithelial cells through downregulating let-7i. *Human immunology*, *75*(8), 760-765.
32. Yasukawa, H., & Yagita, K. (2010). Silent information regulator 2 proteins encoded by Cryptosporidium parasites. *Parasitology research*, *107*(3), 707-712.
33. Veiga-Santos, P., Reignault, L. C., Huber, K., Bracher, F., Souza, W. D., & Ulisses De Carvalho, T. M. (2014). Inhibition of NAD+-dependent histone deacetylases (sirtuins) causes growth arrest and activates both apoptosis and autophagy in the pathogenic protozoan Trypanosoma cruzi. *Parasitology*, (6), 814-825.
34. Soares, M. B., Silva, C. V., Bastos, T. M., Guimarães, E. T., Figueira, C. P., Smirlis, D., & Azevedo Jr, W. F. (2012). Anti-Trypanosoma cruzi activity of nicotinamide. *Acta tropica*, *122*(2), 224-229.
35. Alsford, S., Kawahara, T., Isamah, C., & Horn, D. (2007). A sirtuin in the African trypanosome is involved in both DNA repair and telomeric gene silencing but is not required for antigenic variation. *Molecular microbiology*, *63*(3), 724-736.
36. Wang, Y. H., Zheng, G. X., & Li, Y. J. (2016). Giardia duodenalis GlSir2. 2, homolog of SIRT1, is a nuclear-located and NAD+-dependent deacethylase. *Experimental parasitology*, *169*, 28-33.
37. Contreras, L. E., Suárez, A. G., Diaz, G. J., & Ramírez, M. H. (2019). GlSir2. 1 of Giardia lamblia is a NAD+-dependent cytoplasmic deacetylase. *Heliyon*, *5*(4), e01520.
38. Religa, A. A., & Waters, A. P. (2012). Sirtuins of parasitic protozoa: in search of function (s). *Molecular and biochemical parasitology*, *185*(2), 71-88.
39. Hailu, G. S., Robaa, D., Forgione, M., Sippl, W., Rotili, D., & Mai, A. (2017). Lysine deacetylase inhibitors in parasites: past, present, and future perspectives. *Journal of Medicinal Chemistry*, *60*(12), 4780-4804.
40. Scholte, L. L., Mourão, M. M., Pais, F. S. M., Melesina, J., Robaa, D., Volpini, A. C., ... & Nahum, L. A. (2017). Evolutionary relationships among protein lysine deacetylases of parasites causing neglected diseases. *Infection, Genetics and Evolution*, *53*, 175-188.
41. Szklarczyk, D., Santos, A., von Mering, C., Jensen, L. J., Bork, P., & Kuhn, M. (2016). STITCH 5: augmenting protein–chemical interaction networks with tissue and affinity data. *Nucleic acids research*, *44*(D1), D380-D384.
42. Szklarczyk, D., Gable, A. L., Lyon, D., Junge, A., Wyder, S., Huerta-Cepas, J., ... & Jensen, L. J. (2019). STRING v11: protein–protein association networks with increased coverage, supporting functional discovery in genome-wide experimental datasets. *Nucleic acids research*, *47*(D1), D607-D613.
43. Waterhouse, A., Bertoni, M., Bienert, S., Studer, G., Tauriello, G., Gumienny, R., ... & Lepore, R. (2018). SWISS-MODEL: homology modelling of protein structures and complexes. *Nucleic acids research*, *46*(W1), W296-W303.
44. Eswar, N., Webb, B., Marti- Renom, M. A., Madhusudhan, M. S., Eramian, D., Shen, M. Y., ... & Sali, A. (2006). Comparative protein structure modeling using Modeller. *Current protocols in bioinformatics*, *15*(1), 5-6.
45. Ko, J., Park, H., Heo, L., & Seok, C. (2012). GalaxyWEB server for protein structure prediction and refinement. *Nucleic acids research*, *40*(W1), W294-W297.
46. Benkert, P., Biasini, M., & Schwede, T. (2011). Toward the estimation of the absolute quality of individual protein structure models. *Bioinformatics*, *27*(3), 343-350.
47. Prisant, M. G., Richardson, J. S., & Richardson, D. C. (2003). Structure validation by Calpha geometry: Phi, psi and Cbeta deviation. *Proteins*, *50*, 437-450.
48. Berjanskii, M., Zhou, J., Liang, Y., Lin, G., & Wishart, D. S. (2012). Resolution-by-proxy: a simple measure for assessing and comparing the overall quality of NMR protein structures. *Journal of biomolecular NMR*, *53*(3), 167-180.
49. Wallner, B., & Elofsson, A. (2003). Can correct protein models be identified?. *Protein science*, *12*(5), 1073-1086.
50. Wiederstein, M., & Sippl, M. J. (2007). ProSA-web: interactive web service for the recognition of errors in three-dimensional structures of proteins. *Nucleic acids research*, *35*(suppl_2), W407-W410.
51. Laskowski, R. A., Jabłońska, J., Pravda, L., Vařeková, R. S., & Thornton, J. M. (2018). PDBsum: Structural summaries of PDB entries. *Protein science*, *27*(1), 129-134.

52. Vajda, S., Yueh, C., Beglov, D., Bohnuud, T., Mottarella, S. E., Xia, B., ... & Kozakov, D. (2017). New additions to the C lus P ro server motivated by CAPRI. *Proteins: Structure, Function, and Bioinformatics*, *85*(3), 435-444.
53. Kozakov, D., Hall, D. R., Xia, B., Porter, K. A., Padhorny, D., Yueh, C., ... & Vajda, S. (2017). The ClusPro web server for protein–protein docking. *Nature protocols*, *12*(2), 255-278.
54. Kozakov, D., Beglov, D., Bohnuud, T., Mottarella, S. E., Xia, B., Hall, D. R., & Vajda, S. (2013). How good is automated protein docking?. *Proteins: Structure, Function, and Bioinformatics*, *81*(12), 2159-2166.
55. Weng, G., Wang, E., Wang, Z., Liu, H., Zhu, F., Li, D., & Hou, T. (2019). HawkDock: a web server to predict and analyze the protein–protein complex based on computational docking and MM/GBSA. *Nucleic acids research*, *47*(W1), W322-W330.
56. Genheden, S., & Ryde, U. (2015). The MM/PBSA and MM/GBSA methods to estimate ligand-binding affinities. *Expert opinion on drug discovery*, *10*(5), 449-461.
57. Laskowski, R. A., & Swindells, M. B. (2011). LigPlot+: multiple ligand–protein interaction diagrams for drug discovery. *Journal of chemical information and modeling*. 51(10):2778-2786.
58. Zhang, C., Freddolino, P. L., & Zhang, Y. (2017). COFACTOR: improved protein function prediction by combining structure, sequence and protein–protein interaction information. *Nucleic acids research*, *45*(W1), W291-W299.
59. Roy, A., Yang, J., & Zhang, Y. (2012). COFACTOR: an accurate comparative algorithm for structure-based protein function annotation. *Nucleic acids research*, *40*(W1), W471-W477.
60. Van Der Spoel, D., Lindahl, E., Hess, B., Groenhof, G., Mark, A. E., & Berendsen, H. J. (2005). GROMACS: fast, flexible, and free. *Journal of computational chemistry*, *26*(16), 1701-1718.
61. Schmid, N., Eichenberger, A. P., Choutko, A., Riniker, S., Winger, M., Mark, A. E., & van Gunsteren, W. F. (2011). Definition and testing of the GROMOS force-field versions 54A7 and 54B7. *European biophysics journal*, *40*(7), 843-856.
62. Cassandri, M., Smirnov, A., Novelli, F., Pitolli, C., Agostini, M., Malewicz, M., ... & Raschellà, G. (2017). Zinc-finger proteins in health and disease. *Cell death discovery*, *3*(1), 1-12.
63. Zhang, W., Xu, C., Bian, C., Tempel, W., Crombet, L., MacKenzie, F., ... & Qi, C. (2011). Crystal structure of the Cys2His2-type zinc finger domain of human DPF2. *Biochemical and biophysical research communications*, *413*(1), 58-61.
64. Gray, K. A., Yates, B., Seal, R. L., Wright, M. W., & Bruford, E. A. (2015). Genenames. org: the HGNC resources in 2015. *Nucleic acids research*, *43*(D1), D1079-D1085.
65. Klug, A. (1999). Zinc finger peptides for the regulation of gene expression. *Journal of molecular biology*, *293*(2), 215-218.
66. Laity, J. H., Lee, B. M., & Wright, P. E. (2001). Zinc finger proteins: new insights into structural and functional diversity. *Current opinion in structural biology*, *11*(1), 39-46.
67. Matthews, J. M., & Sunde, M. (2002). Zinc fingers- - folds for many occasions. *IUBMB life*, *54*(6), 351-355.
68. Brown, R. S. (2005). Zinc finger proteins: getting a grip on RNA. *Current opinion in structural biology*, *15*(1), 94-98.
69. Hall, T. M. T. (2005). Multiple modes of RNA recognition by zinc finger proteins. *Current opinion in structural biology*, *15*(3), 367-373.
70. Gamsjaeger, R., Liew, C. K., Loughlin, F. E., Crossley, M., & Mackay, J. P. (2007). Sticky fingers: zinc-fingers as protein-recognition motifs. *Trends in biochemical sciences*, *32*(2), 63-70.